7-19-2022

Modeling and Analysing the Impact of Heat Pump Water Heaters on Distribution Systems Using GridLAB-D

Midrar Adham

Portland State University

Modeling and Analysing the Impact of Heat Pump Water Heaters on Distribution Systems Using GridLAB-D

by

Midrar Adham

A thesis submitted in partial fulfillment of the
requirements for the degree of

Master of Science
in
Electrical and Computer Engineering

Thesis Committee:
Robert Bass, Chair
John Acken
Mahima Gupta

Portland State University
2022

Abstract

With the constant increase in energy demand, finding ways to reduce peak load and the energy-costs factors has become more imperative. Domestic water heating showcases a significant opportunity for such applications. Water heating is the second-highest energy consumer in the residential sector across the United States. Electric Water Heaters (EWHs), in particular, constitute nearly 43% of American household water heating energy consumption. Heat Pump Water Heaters (HPWHs), on the other hand, are an advanced water heating technology that has recently emerged in the United States residential market.

The objectives of this work are to develop a HPWH model and build a case study that evaluates various penetration levels of HPWH in providing reduced peak load and cost-effective energy savings for both utilities and customers. The HPWH model was developed and integrated within the GridLAB-D simulation environment. The model behavior was then validated against a real HPWH unit at Portland State University (PSU).

The case studies incorporated five HPWH penetration levels, ranging from 20% to 100%. In each case, EWHs were replaced with HPWHs. The results showed that a high penetration level of HPWHs can reduce the energy consumption on a distribution system to 38%.

Dedication

To my family and E.L.

Acknowledgements

First and foremost, I would like to express my profound gratitude to Dr. Robert Bass, my advisor, and mentor, for his unwavering support, continuous guidance, and endless patience during my undergraduate and graduate degrees. Without his intellectual insights, this work and others would not have been possible. It's been a pleasure to work with you and be part of your team.

I would like to acknowledge my current and former colleagues. To Mohammed Alsaid, thank you for being my valuable resource in programming and for your support in all aspects of my graduate degree. My gratitude is also extended to Abdullah Barghouti, Shahad Alomani, Dr. Obi, Sean Keene, and Jacob Sheeran for making this journey easier and more enjoyable.

I am indebted to my beloved parents and siblings, Mohannad, Moayad, Shahad, and Leen. Your encouragement, love, and support during my study have sustained me this far. Also, I would like to thank my friends, Mahmoud Abdulqader and Mohammed Almowri, for their help and motivation during my academic career.

Finally, thank you to my thesis committee, Dr. John M. Acken and Dr. Mahima Gupta, for the time they have shared with me. Dr. Acken, thank you for your valuable lessons last year. These literature review sessions helped me become a better researcher.

Contents

List of Tables

List of Figures

Acronyms

ABM Agent-Based Modeling

BESS Battery Energy Storage System

CFD Computational Fluid Dynamics

COP Coefficient of Performance

CSV Comma-Seperated Values

CTA Consumer Technology Association

DCS Distributed Control System

DER Distributed Energy Resource

DG Distributed Generation

DLC Direct Load Control

DoE Department of Energy

DR Demand Response

DSM Demand Side Management

EIA Energy Information Administration

ELCAP End-Use Load and Consumer Assessment Program

EMCB Energy Management Circuit Breaker

EPRI Electric Power Research Institute

ETP Equivalent Thermal Parameter

EUS Energy Utility Systems

EV Electric Vehicle

EWH Electric Water Heater

FBS Forward-Backward Sweep

GHG Greenhouse Gas

GPM Gallon Per Minute

GUI Graphical User Interface

HELICS Hierarchical Engine for Large-scale Infrastructure Co-Simulation

HP Heat Pump

HPWH Heat Pump Water Heater

HVAC Heating Ventilation and Air Conditioning

IoT Internet of Things

NEEA Northwest Energy Efficiency Alliance

NR Newton Raphson

NRECA National Rural Electric Cooperative Association

NREL National Renewable Energy Laboratory

NRMSE Normalized Root Mean Square Error

OpenDSS Open Distribution Simulator Software

PGE Portland General Electric

PNNL Pacific Northwest National Laboratory

PSH Pumped Storage Hydropower

PSU Portland State University

PTR Peak Time Rebate

PV Photovoltaic

RBSA Residential Building Stock Assessment

RER Renewable Energy Resource

SCOP Seasonal Coefficient of Performance

SEER Seasonal Energy Efficiency Ratio

SOA Service Oriented Architecture

SOLC Service-Oriented Load Control

TCL Thermostatically-Controlled Load

TMY Typical Meteorological Year

ToU Time of Use

UCM Universal Communication Module

1 Introduction

1.1 Problem Statement

With the constant increase in energy demand, finding ways to reduce peak load and the energy-cost factors associated with it has become more imperative. For decades, the bulk power system generated, transmitted, and delivered electricity to customers reliably through conventional generators. However, the global transition toward clean energy enabled the integration of Renewable Energy Resources (RERs), thereby render the use of traditional, fossil-fuel power plants less sensible in light of climate change concerns. Wind and solar, for instance, have been commonly utilized, whether by grid service providers as a utility-scale generation or by small residential and commercial sectors as distributed generation. RERs are weather dependant, and as the weather changes its course throughout the day, RER become less effective. This stochastic behavior creates significant obstacles for grid operators to maintain the balance between supply and demand.

Despite the intermittent nature of RERs, their deployment is still emerging due to environmental concerns [1]. Therefore, the issues associated with the integration of RERs can be addressed by the utilization of advanced storage systems or emphasizing the control on the demand side, known as Demand Side Management (DSM). Advanced storage systems, such as Pumped Storage Hydropower (PSH) and Battery Energy Storage Systems (BESSs), can be used to store energy when RERs generate electricity and dispatched during peak demand period. However, the lack of geographical locations of the former and the latter's high cost make them currently not viable on a large scale. DSM, on the other hand, provides means of maintaining energy balance by controlling customer-owned Distributed Energy Resources (DERs) to provide grid services in real time. Energy-storage and high power consumption DERs, such as water heaters, are ideal candidates for DSM programs. This work evaluates the significance of Heat Pump water heaters in providing reduced peak load and cost-effective energy savings for both utilities and customers.

1.2 Work Objectives

Water heating is the second-largest energy consumer in the residential sector. According to the U.S Energy Information Administration (EIA), 18% of typical home energy usage is consumed by water heating. While 97% of U.S homes use various types of water heaters, including gas storage and tankless, a significant share is of EWHs, which account for approximately 43% as shown in Figure 1.1 [2]. Once triggered, the average EWH draws 4.5 kW.

HPWHs are more energy-efficient devices and various federal laws have been passed to encourage their deployment as EWHs alternatives. In fact, HPWHs are expected to reach 31% of residential market share by 2039 [3]. This research characterizes the potential benefits of HPWHs as an alternative to EWHs. For that aim, a case study is developed that incorporates a 13 Node Feeder model using GridLAB-D simulation platform.

GridLAB-D is an open-source, power distribution system simulation tool that was developed by the U.S Department of Energy (DoE) at Pacific Northwest National Laboratory (PNNL) [4]. Among other modules, GridLAB-D incorporates a residential module. The residential module facilitates end-use loads such as water heaters and houses. Two water heater models currently exist in GridLAB-D, an EWH and a HPWH. While testing the HPWH model, it was shown that certain parameters are randomly calculated, and consequently, simulate an inappropriate behavior of HPWHs. Therefore, for this thesis, a HPWH model was developed and integrated within GridLAB-D source code. Further, the model behavior was validated against a real HPWH unit. Testing was conducted to ensure that the developed HPWH model in this thesis is able to interact with other modules within GridLAB-D, such as climate and market modules.

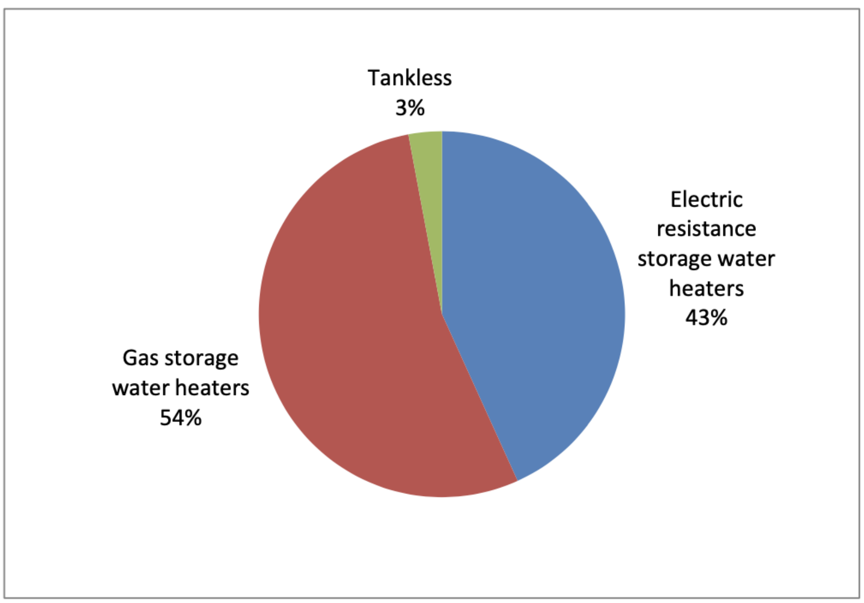

Figure 1.1: Percentage of Different Types of Water Heaters Used in The Residential Sector [2].

2 Literature Reerbaiew

2.1 Demand Side Management

Technological advancements in communications and smart grid protocols have enabled novel various approaches to enhance grid reliability and stability. Owing to these advancements, routinely-used household appliances such as water heaters, and newly emerged loads including Photovoltaics (PVs) and Electric Vehicles (EVs), have become grid-interactive. Even though such loads provide high variability to the demand profile, they can be utilized to provide substantial contributions to grid reliability. For instance, water heaters can be remotely managed to turn ON/OFF, and inverters can provide functions such as Frequency-Watts and Volt-VAr curve controls [5]. Generally, these loads are customer-owned storage assets. When aggregated, they can provide a MW scale impact within a balancing area [6]. Therefore, utilities have developed several programs to deploy such loads in grid services. The broader name for these programs is Demand Side Management (DSM).

DSM refers to utilities' programs that are designed to manage customers' energy use during peak demand periods. These programs range from permanent improvements in energy efficiency (energy-efficient appliances. i.e HPWH) to real-time control of customers' DERs. The latter falls under the category of a more specific type of DSM, which is Demand Response (DR). Both DSM and DR programs are driven by economic incentives for both residential and commercial sectors to encourage customers to participate in DSM programs and reduce their energy consumption [7].

2.1.1 Traditional Approach

Utilities have developed several DR strategies to employ DERs in grid services. These strategies can be divided into two categories: price-based programs and incentive-based programs. Price-based programs reflect the real-time energy prices based on the availability of supply resources [8]. The Portland General Electric (PGE) Peak Time Rebate (PTR) program, for instance, notifies enrolled customers of PGE peak-load periods, three hours each. Customers may choose to participate in these events by reducing their loads. If they do, PGE compares the customers' power usage during the peak-load period with the previous 10 days in the same time, creating a baseline case. Customers then receive a financial rebate of $1 per 1 kWh of load reduction compared to the baseline case.

In contrast to allowing customers to choose their participation, some DR programs operate by utilizing Direct Load Control (DLC) of customers' assets. In DLC, customers' DERs are fully controlled by the utility during a period of its choosing, regardless of customers preferences [9]. DLC programs have been around for decades. They are the most common strategy in DR programs [10]. In 1970, a small scale DLC study was implemented due to the increased penetration of air conditioners, and financial incentives were offered in return [10]. On a large scale, however, Florida Power implemented a large study that included water heaters, pool pumps, and centeral heating systems in 1979 [11]. Since then, DLC programs have enabled aggregation of DERs to provide DR peak load shifting and peak load mitigation.

2.1.2 Modern Approach

Both of the previously mentioned types of DSM present challenges that adversely impact the enrollment scope of DR programs. DLC sets constraints on customers' DERs operation. In other words, customers have to give up control of their DERs for a period of time that is specified by the utility. Time of Use (ToU) and PTR programs require customer diligence. A successful DR program incorporates a large population of DERs. As such, maintaining customer comfort and enrollment is a priority. Therefore, modern approaches of DR programs provide customers with a greater degree of freedom to choose whether to participate or opt out from DR programs. Further, modern approaches provide means for DER to interface with the program without yielding control to the utility.

Service-Oriented Load Control (SOLC) is a modern approach in DSM programs. SOLC is based on Service Oriented Architecture (SOA) that allows entities to exchange information within an Internet of Things (IoT) network [12, 13]. From an energy management perspective, SOLC provide means of information exchange between a utility and its customers. As illustrated by Slay and Bass [14], a cloud-based assessor, provided by the utility, seeks customer permission to determine the value of their DER, without including private information, such as DER profile or its behavior. Once permission is granted, the utility provides the customer with a set of grid services based on the previous assessment. The customer then chooses the appropriate grid service that they wish to execute, thereby making the DER available for the utility to dispatch. Further, customers may interact with the utility to override a service request. Therefore, SOLC allows the customer to retain the choice to participate in grid services and have full control over their DER.

2.2 Heat Pump Water Heaters

The term HPWH is used interchangeably in the literature. While in some cases, it refers to a stand-alone heat pump system added to an EWH, in other cases, it refers to fully integrated equipment that includes a heat pump and a water heater. In this work, the term HPWH will be used hereafter to refer to fully-integrated equipment.

Even though HPWHs are considered new technology emerging to the U.S market, their development goes back to 1935 [15]. The National Rural Electric Cooperative Association (NRECA) and DoE provided a grant to Energy Utility Systems (EUS) to develop a HPWH prototype. The EUS manufactured 100 HPWH models, 85 of these models were fully assembled units, and the rest were individual heat pump systems to be integrated with existing EWHs. Due to high maintenance costs and excessive noise, the HPWH market collapsed and less units were sold during the mid 1990s [16].

The advancements in technology and manufacturing in the 20th century solved many of the issues mentioned previously. HPWHs are now more convenient and cost less. Furthermore, in line with energy conservation requirements, federal water-heating standards require water heaters that are larger than 50 gallons to have an energy factor of ≈ 2, which is easily achieved by HPWHs. A National Renewable Energy Laboratory (NREL) study reported that

HPWHs could provide a significant reduction in energy consumption and cost savings [15]. The study estimated that if all EWHs were replaced with HPWHs, water heater operating costs could be reduced by $182 per household and annual energy consumption by 0.7 quads.

2.2.1 Operation Principle

Like a refrigerator or an air conditioner, but in a reverse cycle, HPWHs work by moving heat from the surrounding air to heat the water in the tank. As the air is absorbed to the device, it goes through an evaporator. The evaporator contains a refrigerant that pulls the heat from the absorbed air. A compressor then compresses the refrigerant, which causes its temperature and pressure to increase. The refrigerant passes through condenser coils that transfer the heat to the water in the tank. This process is known as vapor-compression cycle.

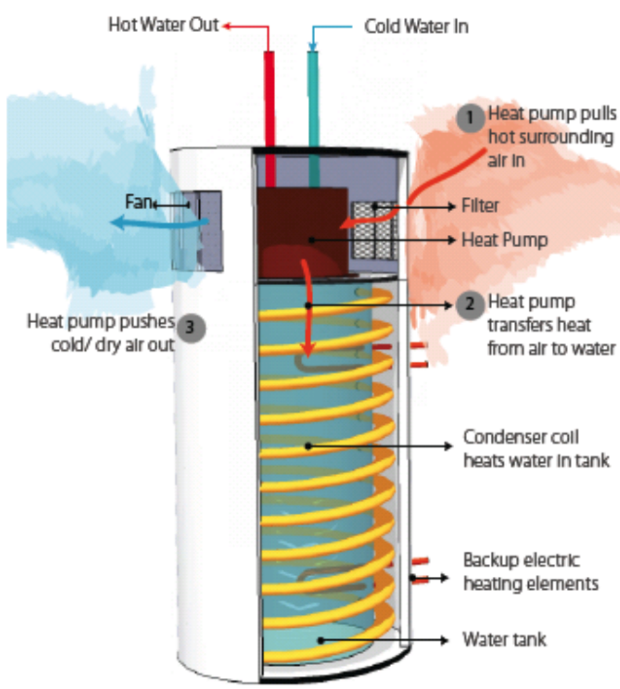

Figure 2.1: HPWH Principle of Operation [15]

As shown in Figure 2.1, HPWHs are equipped with two heating sources, primary and secondary. The primary heating source is the compressor, and its rated power ranges between 400 W - 1000 W, depending on the tank size. The secondary heating source consists of two backup resistive elements, each rated for 4.5 kW for 50 gallons in size or larger tanks. Generally, the operation priority of each heating source depends on the water draw volume and the device internal control logic [9, 17]. The performance of HPWHs is evaluated by the Coefficient of Performance (COP). The COP is the ratio between the transferred heat energy by the heat pump system to the tank and the consumed energy by the source. HPWHs can easily achieve a COP of 2 under normal weather conditions, compared to $\approx$ 0.98 for EWHs.

Because of their controlling logic, HPWHs take far more time to switch ON and OFF compared to EWHs. Several studies showed that HPWHs take more than 140 seconds to trigger, whether to respond to a DR signal or change in the water temperature [3, 9]. EWHs, on the other hand, respond to such events in less than 3 seconds [3]. These characteristics adversely reflect on HPWHs role as DR assets, which will be discussed in the following section.

2.3 Water Heaters in Demand Response

Aside from this prevailing population of EWHs, they have unique characteristics that leverage them to be primary candidates for DR programs. Once heated, tank-type water heaters maintain the water temperature for a period of time, acting as energy storage devices. This can be used to provide grid services such as peak load shifting. Further, the EWH heating source is simply a resistor. This fact qualifies EWHs to suit grid services needs for the following reasons:

- Unlike induction loads, purely resistive loads eliminate the need for reactive power support from the grid.
- The resistor eliminates the lockout time needed for heat pump-based devices (i.e air conditioner and HPWH) after multiple switching actions [18].

Also, their control logic is quite simple, which makes them quick to respond to utility signals regarding switching ON or OFF. These characteristics leverage EWHs to be used for peak load mitigation and frequency response services.

HPWHs are not the preferable option for some grid services, such as Frequency Response. Unlike EWHs where the heating source triggers immediately when needed, HPWHs follow a determined sequence of processes set by the manufacturer to decide which heating source to trigger [9]. This decision-making process takes time, during which grid problems might exacerbate.

Generally, water heaters are mainly driven by hot water draws, which means that customers' hot water needs decide the shape of the demand profile of these devices. Therefore, maintaining the water temperature within customers' comfort level is a priority for a successful DR program. Adham et al. explored the implications of DLC control using a HPWH and EWH [9]. The results reported a significant drop in the water temperature due to de-energizing the water heaters during peak demand periods. This indicates that much less hot water is available for DERs' owner. Such water heaters behavior could result in less customers enrollment in DR programs. A similar study, but on a large scale, recruited over 150 households with an average of 2.9 people in each home [17]. The study period was six weeks, wherein peak load shaving and peak load shifting results were analyzed and assessed weekly. During the study period, specifically after load shaving events, several customers were not satisfied with the performance of their DERs and, therefore, decided to opt-out from the study.

2.4 Modeling Approaches

The performance of HPWH is largely affected by the ambient temperature of the surrounding environment. NREL carried out a study on several HPWHs devices installed in different geographical locations in the United States. One unit, in particular, was installed in a basement with ambient temperature below $50°F$ [15]. The performance of this unit was monitored during the winter season, from December to April. The resistive heating element was frequently used instead of the compressor due to low ambient temperature. Furthermore, another study conducted by NREL on five HPWHs across the United States [19]. Some of the HPWH units were installed in an unconditional space that has a low ambient temperature, below $57°F$. While monitoring the performance of these units, NREL reported that the HPWHs switched to the resistive heating elements due to icing on the evaporator coils.

Modeling such aspects can be complex and require extensive labor work and expenses. Therefore, researchers tend to use different approaches to model HPWHs. These approaches can be categorized as follows: equation fit approach and deterministic approach [20]. The first modeling method requires either information from the manufacturer or monitoring the unit's behavior in certain conditions. The latter, however, considers each component of the refrigeration system, such as the compressor, evaporator, and condenser. This section will explore both modeling approaches in the literature and evaluate their results.

2.4.1 Deterministic Approach

Fan and Furbo investigated the heat transfer of a hot water tank during standby loss periods [21]. They developed a Computational Fluid Dynamics (CFD) model to calculate temperature stratification in a uniform tank. The results were compared with measurements obtained from a lab experiment to validate the model. Even though the CFD model has some limitations, such as tank size, it predicted the temperature of the stratified layers in the tank closely.

Lee et al., on the other hand, used a genetic algorithm to develop a heat exchanger model [22]. By optimizing the design parameters of the heat exchanger model, they were able to maximize the Seasonal Energy Efficiency Ratio (SEER) and Seasonal Coefficient of Performance (SCOP). Further, the operating parameters considered in their model include outdoor temperature and indoor and outdoor airflow rates.

2.4.2 Equation-Fit Approach

The behavior of HPWH device can be simulated using a curve fit modeling approach. F. Augilar et al. carried out several test cases to develop a mathematical HPWH model. All experiments were conducted in a $19°C$ - $23°C$ ambient temperature environment and with 55$\degree C$ inlet water temperature. The mathematical model was implemented in two steps to capture the tank stratification and the behavior of the refrigeration system. The mathematical model performance was validated against one-year experimental results. The model successfully simulated the HPWH tank stratification with a $2.6\degree C$ error. Additionally, the deviation between the rated COP and the simulated COP is 5.1%.

For a GridLAB-D model that comprises a large number of loads or long simulation periods, one may seek efficient and simple yet representative load models to reduce the simulation time and accurately capture the device behavior. The methods mentioned above are implemented with algorithms that may require high computational requirements and increase the simulation time. Therefore, this work aims to provide a simplified HPWH model using an equation-fit modeling approach. A lab test station that incorporates a HPWH unit is used to validate the model results. The proposed model considers a variety of the HPWH unique characteristics, including the heating sources switching and the device COP. Further, a case study is developed that uses a 13 node feeder with 1000 houses to study the impact of HPWHs on a distribution system.

2.5 Power Simulation Tools

The advent of Distributed Generation (DG) resources and DER integration is redefining the grid operation status quo. Instead of a one-way power flow paradigm, from transmission to distribution networks, these resources inject power upstream. On one hand, this paradigm-shifting poses challenges to grid operators and planners, such as voltage disturbances and transformer overloading due to EVs charging [23]. On the other hand, DERs provides ancillary services such as peak load mitigation and shifting to release the stress on grid components during peak periods. As well, DGs, if integrated appropriately, may be used as decentralized generation assets to reduce Greenhouse Gass (GHGs) emitted from traditional fossil-fuel generators.

The behavior of the resources mentioned above and their integration into the local grid is complex by nature. Advanced simulation platforms are required to evaluate the benefits and issues within transmission and distribution networks. Various software packages have been developed to help grid operators and academia investigate such aspects. This Section discusses two simulation software packages that are most suitable for analyzing the impact of DERs on distribution and transmission systems.

2.5.1 OpenDSS

Open Distribution Simulator Software (OpenDSS) is an open-source power system tool developed to perform distribution system analysis. Electrotek Concepts initially designed it in 1997. In 2008, Electric Power Research Institute (EPRI) acquired the software and made it publicly available [24]. OpenDSS is widely used by utilities and researchers for the following reasons. First, it supports power flow analysis, harmonic analysis, capacitor bank control, and short circuit analysis. Second, its flexibility allows for third-party software integration, such as MATLAB and Python. Finally, it supports distributed generation analysis, including EVs and PVs. A compelling feature in OpenDSS that distinguishes it from other open-source software tools is that it can be extended to be more user-friendly.

For example, a DSSView processor program can be integrated within OpenDSS to offer a Graphical User Interface (GUI).[1]

2.5.2 GridLAB-D

GridLAB-D is another open-source power system simulation tool that has similar features as OpenDSS. GridLAB-D was developed by PNNL, a laboratory within the U.S DoE, in 2008. Among others, GridLAB-D distinguishes itself by incorporating several modules that facilitate the aspects of DR programs, integration of DERs and RERs including PV and wind turbines, and energy markets [4]. Furthermore, GridLAB-D features two algorithms used for distribution and transmission systems analysis. The Forward-Backward Sweep (FBS) solver is mainly used for radial systems such as IEEE four and 13 Node test feeders, while the Newton Raphson (NR) solver is used for loop systems [25].

The interactions between transmission and distribution systems are discussed for optimization and planning purposes. In certain case studies, one might seek to model a regional network incorporating different topologies, such as radial or loop networks. Such a large system requires multi-solvers running simultaneously. GridLAB-D's flexibility allows it to perform such co-simulation using the Hierarchical Engine for Large-scale Infrastructure Co-Simulation (HELICS) environment. HELICS enables the integration of several simulation software packages such as PowerWorld, PSSE, and GridLAB-D, with GridLAB-D to perform a large-scale analysis.

[1] Sourceforge. Roger Dugan, OpenDSS Developer.

GridLAB-D is capable of simulating a variety of DLC strategies. For example, a DER such as a water heater may interact with energy market pricing signals. By incorporating a market module, the water heater turns off during high energy prices and turns back on during low energy prices. Additionally, GridLAB-D features implicit and explicit end-use loads. If the user chooses implicit house appliances, GridLAB-D runs a set of load profiles that were collected as part of a End-Use Load and Consumer Assessment Program (ELCAP) case study. This allows for a variation in the load profiles for each modeled house. However, explicit end-use loads enable the user to define an individual appliance within a house. Since a specific parameter drives each end-use load, an external load profile can easily be incorporated within the object. For instance, a water draw profile may be used within a water heater object where the object behaves accordingly.

GridLAB-D was chosen over OpenDSS for several reasons. First, unlike OpenDSS, GridLAB-D is compatible with Windows and Unix-based operating systems such as Linux and macOS. Second, GridLAB-D is C++/C based, while OpenDSS is Delphi based, which is not as mainstream as C or C++. Third, GridLAB-D offers very detailed end-use loads that incorporate a climate module. This feature allows users to simulate Heat Pump (HP) and HPWH systems that behave differently in various weather conditions.

3 Design Methodology

3.1 Design Considerations

One of the goals of this work is to evaluate the impact of HPWHs deployment on distribution systems using the GridLAB-D modeling environment. The case study uses an IEEE-13 Node test feeder with 1000 household profiles populated over the appropriate nodes. Each node incorporates several end-use loads, representing a household typical load profile and a water heater. The IEEE-13 Node test feeder design and loads distribution were inherited from S. Alomani's work [23]. However, some modifications were needed, given the nature of the work presented here.

Initially, the idea was to use the existing water heater models within the GridLAB-D models library. However, upon testing the HPWH model, it was discovered that it behaved unexpectedly. Several water heater properties seemed to be randomly changing, such as the water temperature, tank state, and water heater model. Therefore, a HPWH model was developed and validated against a physical HPWH unit. The physical HPWH unit is part of a water heater station located at Portland State University.

Given the fact that the new HPWH model will be included within GridLAB-D, a review of GridLAB-D source code was required. A secondary objective of the HPWH model is to achieve a low overhead of simulation time. In other words, the simulation time of a given test feeder that includes EWHs should be the same as a similar feeder that uses HPWHs instead. Therefore, most of the defined variables in the source code for other end-use loads such as EWH, Heating Ventilation and Air Conditioning (HVAC) systems, and refrigerator models were used instead of introducing new variables.

3.2 Water Heater Test Station

The water heater test station is located at Portland State University (PSU)'s Power Lab. It constitutes various components that facilitate the automation of water draw events, scheduling CTA-2045 services, and energy measurements. These components include, but are not limited to, flow meters, valves, current transducers, and serial communications. In this work, however, only the relevant aspects of the HPWH are discussed. Any further information may be procured from thesis work by L. Clarke [3] and A. Clarke [26] who largely contributed to building, setup, and testing the water heater test station.

3.2.1 Distributed Control System and CTA-2045

The goal of the Consumer Technology Association (CTA)-2045 standard is to further enable end-use loads to be deployed in DR programs. The standard defines a port interface that can be designed by the end-use load manufacturer, so the device is ready for energy management and control applications. According to the end-use load type and characteristics, the manufacturer may then choose what commands to implement and provide appropriate responses when queried. Further, utilities can build a Universal Communication Module (UCM) that translates incoming instructions to CTA-2045-equivalent commands. EPRI provided a C++ library and example applications that facilitate all CTA-2045 commands and queries.

Generally, the CTA-2045 commands, by design, do not turn off the water heaters completely. They, instead, have windows of operation relative to the thermal energy available within the tank. The minimum and maximum thresholds for each window are specified by the manufacturer. A set of CTA-2045 commands and queries that were frequently used in this work are *load up, grid emergency, and commodity read*. Therefore, the following Section elaborates on the use of these commands and highlights the corresponding changes in the HPWH characteristics.

For this work, one may interface with the HPWH by exchanging CTA-2045 commands or queries its information with the Distributed Control System (DCS). For each command sent to the HPWH, a response is received and logged by the DCS. The DCS records these responses in a Comma-Seperated Values (CSV) file, which can be later used for further analysis. For instance, a *load up* command instructs the HPWH to turn on immediately to heat the water to the specified set point. The *grid emergency* command, on the other hand, lowers the thermostat set point such that it uses minimal energy regardless of hot water availability (not recommended and rarely used). The *commodity read* query reports the HPWH status including *EnergyTake* in Watts-hour (Wh), *cumulative energy* (Wh), and power consumption in Watts (W). Note that the power consumption is not implemented within CTA-2045; it was rather included within the DCS by the Portland State University team. The DCS also sends non-CTA-2045 commands and queries to the water heater test station, including immediate or scheduled water draw events.

3.2.2 Heat Pump Water Heater Physical Unit

The water heater test station comprises two grid-enabled, A. O. Smith, 50 gallon water heater units: an Electric Water Heater (EWH)[2], and a Heat Pump Water Heater (HPWH)[3]. Both water heater units are designed with upper and lower resistive heating elements, each rated for 4.5 kW. The HPWH has an additional HP system, where the compressor is rated for 1.7 A, resulting in 410 W when triggered. Furthermore, the HPWH has a front panel that allows users to enable/disable remote access, change the temperature setpoint, and switch the mode of operation.

The HPWH has four modes of operation, Electric, Efficiency, Hybrid, and Vacation. Each mode restricts the device to certain characteristics and decides its behavior. For instance, in Electric mode, the device runs as an EWH, thereby triggering only the resistive heating elements and locking the HP operation. In Efficiency mode, however, the burden is entirely on the HP during normal conditions. The Hybrid mode is where both resistive heating elements and HP share the burden of heating the water within the tank. The operation of each heating source is decided by an internal controlling logic that will be detailed in Section 3.2.3. Finally, the Vacation mode sets the maximum temperature threshold to $60°F$ and disables remote access to the unit. This mode is used when the unit is not expected to be used frequently, so the HPWH heating sources are less likely to trigger.

[2] 100286470 Electric Resistance Water Heater by A.O. Smith
[3] 100276170 Heat Pump Water Heater by A.O. Smith

3.2.3 Heat Pump Water Heater Controlling Logic

The *EnergyTake* is the amount of energy that the HPWH would need to consume to heat the water in its tank to the temperature set point. Generally, when a water heater is in idle mode, it slowly loses energy. This is known as “idle losses” and results in a gradual increase in *EnergyTake*. *EnergyTake* increases rapidly when a water draw occurs, wherein hot water is removed from the tank and replaced with cold water from the household water supply. *EnergyTake* decreases when the water heater energy source turns on, and it is zero when the tank temperature equals the temperature set point, shown in Figure 3.1.

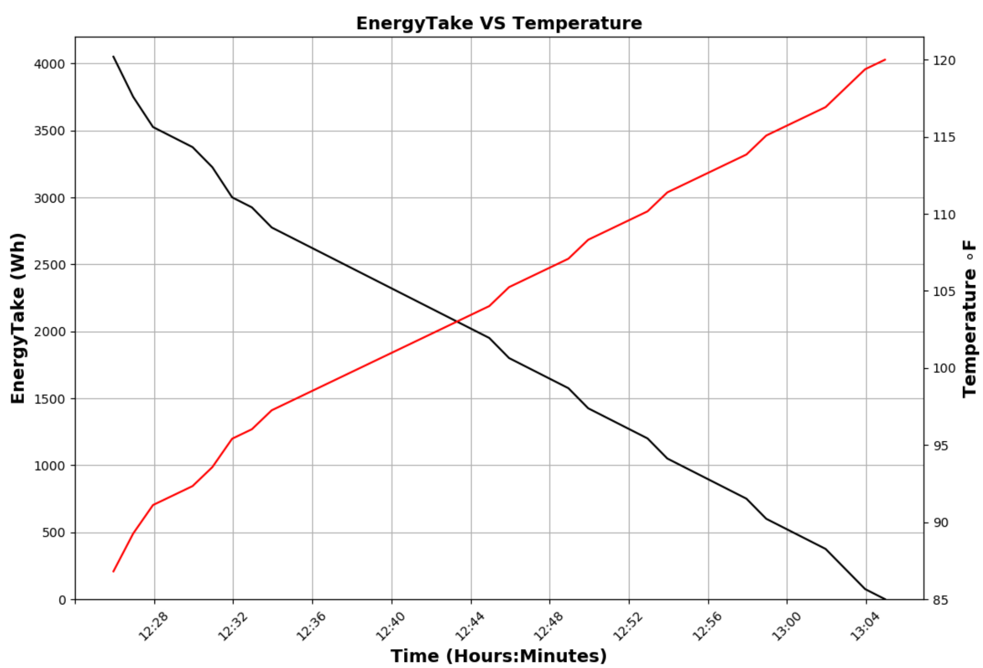

Figure 3.1: Temperature and *EnergyTake* Relationship During Heating Operation

Upon observations, it was noted that the *EnergyTake* thresholds points are the same, regardless of the operation mode [3]. The HPWH switches between heating sources when operated in "Hybrid" mode. In this mode, the compressor triggers when the *EnergyTake* reaches 675 Wh, which then gradually heats the water to the specified setpoint. The resistive heating element, however, triggers only if there is an excessive water draw that causes a sudden and large change in the *EnergyTake*. Once the *EnergyTake* reaches 2000 Wh, the resistive heating element triggers to rapidly heat the water, though not to the specified setpoint. As the *EnergyTake* reaches 1000 Wh, the resistive heating element turns off and, consequently, the compressor triggers to heat the water to the specified setpoint.

3.2.4 Temperature Measurements

As mentioned previously, the water heater test station includes a 50 gallon, A. O. Smith EWH unit. L. Clarke replaced the anode rod of the EWH with five DS18B20 temperature sensors, distributed over the tank [3]. A water draw was then applied to observe the temperature stratification as well as the *EnergyTake*. The sensors report the tank temperature and a CTA-2045 query reports *EnergyTake* values to the DCS, which in turn logs the data in a CSV file in a one-minute time resolution. Figure 3.2 shows the *EnergyTake* behavior as well as the tank temperatures. The sensors are numbered from top to bottom. Though sensors 4 and 5 show a significant temperature drop during a water draw, the three top sensors report less variation in the tank temperature. Note here the *EnergyTake* behavior (reported as "Import Energy") as it increases while the temperature drops. Therefore, the *EnergyTake* can be assumed to reflect the temperature stratification within the lower portion of the tank.

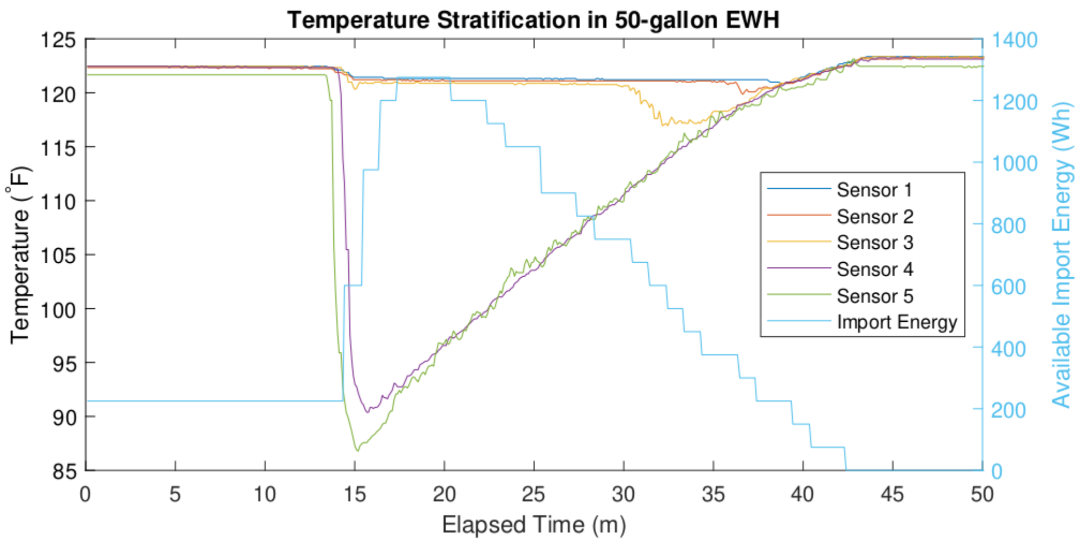

Figure 3.2: Temperature and *EnergyTake* Relationship in EWH [3]

3.3 GridLAB-D Core

GridLAB-D is an agent-based, open-source, power system simulation software [27]. It incorporates advanced algorithms that are capable of simulating emerging smart grid technologies. Though GridLAB-D focuses on distribution systems, which explains the "D" letter at the end of its name, transmission systems can be modeled to examine multi-level system interactions. In a nutshell, GridLAB-D simulates the interoperation between all physical components within a distribution system [4].

Agent-Based Modeling (ABM) technique is a meaningful way to interpret complex systems such as the power grid and energy markets. The complexity of the power system lies within the interactions between its several entities and components, where all of these entities are linked together. These components may be linked physically, such as generators, transformers, substations, and end-use loads. Or, they may interact by using communication technologies for a DR program. Changing one of these entities might cause a chain of variation in the others and vice versa. ABM deals with major system components as individual agents, each of which comprises a variety of simulated versions of the existing physical system components. [28].

3.3.1 Modules

From energy markets to end-use loads, GridLAB-D includes a variety of modules that simulate several aspects of the power system paradigm, including DR strategies. Generally, each one of these aspects is defined within a module wherein several classes and variables are declared. Modules can be instantiated as a *run-time* class or simply calling the module name at the beginning of a *glm* file, the primary file extension where GridLAB-D models are populated.

A market module, for instance, incorporates an *auction object* that facilitates the bidding interactions between sellers and buyers. The *auction object* allows for buyers and sellers to submit their bidding prices for a period of time, known as a bidding period. Once the bidding period ends, the intersection point between the involved parties' biddings will be selected as shown in Figure 3.3.

Figure 3.3: GridLAB-D *auction object* Clearing Price [29]

The *market module* may be concurrently used with the *residential module* to implement DR strategies, such as price-based controlling method. The *residential module*' main end-use loads are House and Water Heater. Other end-use loads exist within the *residential module*. However, the relevant end-use loads to the HPWH modeling approach are discussed in this work.

3.3.1.1 House Object

The *house object* in GridLAB-D is modeled using the Equivalent Thermal Parameter (ETP) approach [30]. Realistically, houses include appliances that either radiate heat, such as a refrigerator, or are directly impacted by the surrounding temperature, such as a HPWH. Considering these factors when modeling a *house object* may result in a large number of parameters that adversely impact GridLAB-D performance. The usefulness of the ETP approach is that it minimizes the model complexity by converting the thermal parameters into electric parameters. Thus, a simple electric circuit is used to evaluate the heat exchange of the house model, shown in Figure 3.4.

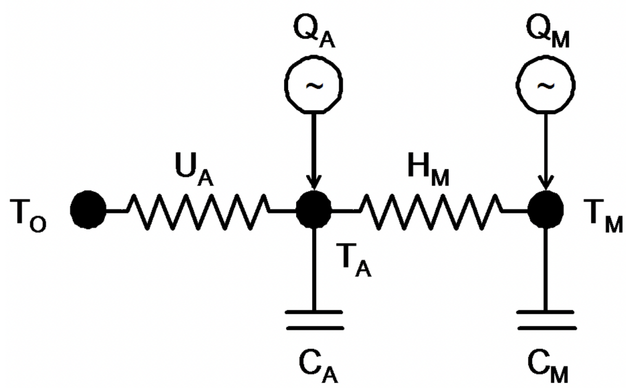

Figure 3.4: GridLAB-D ETP House Equivalent Circuit

GridLAB-D house model is developed by considering the building material thermal conductance, the load geographical location, and the heat radiated from appliances or solar systems to fit the needs of smart grid applications. Thermal conductance is a measure of a material's ability to conduct heat. Since the heat flows through the house structures, including walls, windows, and ceilings, the conductance of these elements is combined and represented in U_A. The same concept is applied to the other parameters in Figure 3.4. The heat gains from the outdoor environment and appliances are lumped together and illustrated as Q_A. Using an electrical engineering analogy, the heat flow is equivalent to the current flow in a circuit, the thermal conductance is the equivalent to resistor elements, and the heat capacity of the building mass and indoor air C_M, C_A are equivalent to capacitor elements.

The house geographical location is a vital aspect considering the nature of the loads modeled in GridLAB-D. Additionally, the operation of Thermostatically-Controlled Loads (TCLs) such as HVAC and water heaters are largely affected by the temperature of their surroundings. These loads are mathematically developed as a function of the outdoor temperature. Therefore, a *climate module* can also be used within a *glm* file along with the *residential module*. The *climate module* uses Typical Meteorological Year (TMY) data set that covers hourly weather data of the United States. The data set is created and maintained by NREL and, in 2008, TMY3 version was released [31].

3.3.2 Water Heater Source Code

The developed water heater models in GridLAB-D are characterized by two resistive heating elements and tanks that are 20 to 100 gallons in size. The water heater switches between two models during simulation, one-node model and two-node model. The one-node model considers the tank at a uniform temperature. The two-node model, however, considers two layers within the tank; each layer is at a uniform temperature. The top layer is nearly equal to the tank set point, and the lower layer is near the inlet water temperature. The two-node model triggers in the occurrence of a water draw or if the tank is being heated.

The amount of the water draw is a critical attribute that defines the tank state, load state, and the water heater model. The tank state may be *full, partial, or empty*. The *full* tank state indicates no water draw or that a relatively small water draw occurred; that is, the temperature of the tank is not affected and is still within its set point. The *empty* state refers to a state where the tank is full of cold water, indicating large amount of hot water was drawn from the tank. Note that the one-node model applies to both of these states. The two-node model appears in the *partial* state, wherein hot water is being drawn from the tank and influx cold water replaces it.

The load state, on the other hand, facilitates the rate of water draw occurrence. Generally, the hot water leaves the top of the tank, whereas cold water enters the lower section of the tank. This effectively triggers the two-node model and the heating element to heat the water. The amount of the water draw is reflected in both the hot and cold water layers within the tank. As the cold layer ascends and reduces the hot layer boundary, the load state changes from *stable* to *depletion*. Note that the upward movement of the cold layer indicates that the heating element was not able to heat the influx water at a quick rate that matches the rate of the influx cold water. Lastly, the *recovering* state infers that water draw occurrence is either negligible or nonexistent, such that the hot water boundary is moving downward.

The aforementioned aspects are the driving parameters for the water heater simulation in GridLAB-D. The load state and tank state are encapsulated within other functions that define different aspects of the water heater. Additionally, the water heater power consumption is a fraction of its parent, if used, which is part of a distribution system. This Section elaborates on the functions used within the water heater source code and explains the methods that GridLAB-D simulation uses to calculate the impacts of the End-use loads and their parents on the rest of the network.

3.3.3 Main Functions

The testing case for this work incorporates several water heaters nested within houses. Each house and each water heater are linked in a "parent-child" relationship, where the parent is the *house* object, and the child is the *water heater* object. This file can be run by invoking the following command in a terminal window:

```
gridlabd [glm file name]
```

GridLAB-D's main entry point resides within a "main.c" file. This file initializes and synchronizes all object instances within the *glm* file. The initialization process calls three functions once per simulation, the *constructor*, *create*, and *init* functions. The *constructor* function publishes the water heater variables. These variables include, but are not limited to, tank characteristics (height, diameter, etc) and water heater properties (set point, thermostat dead-band, etc). Once these variables are published, the *create* function is called where it assigns the published variables to the user inputs and sets default values. For instance, the minimum tank set point allowed is $90°F$. If a lower value were used, the *create* function adjusts the user value to $90°F$. The *create* function sets the developed HPWH model maximum and minimum thresholds for the heating sources. Finally, the *init* function validates the user input values, wherein warnings and errors are displayed if out-of-range values were used.

The synchronization process facilitates the calculation needs for each object within the *residential* module. The GridLAB-D approach uses three methods: a top-down, a bottom-up, and another top-down pass. Each method is encapsulated within a function, a *presync*, a *sync*, and a *postsync*. For instance, the *presync* function performs the top-down method, such that it starts from the parent first then the child (*house* → *water heater*). This process is reversed in the *sync* function. The bottom-up method in the *sync* function determines the water heater (child) needs such as, power consumption, calculates the required parameters, and goes back up to the parent and the rest of the network. Finally, the *postsync* function runs another top-down pass, where it completes the calculations and passes them to the *commit* function wherein objects' states are locked in.

The developed HPWH model is created in a separate function, shown in Section 3.4. This function comprises the necessary calculations and states. Once the calculations are completed within its associated function, it is called in the *postsync* function where the needed parameters are then passed and published.

3.4 Heat Pump Water Heater Model

Unlike the EWH model, the HPWH model follows a determined sequence of operation to trigger a heating source. Identifying this operation and modeling its characteristics are detailed in this Section. Four main dynamics were considered during the modeling process:

- Change in *EnergyTake* during normal operation (idle losses).
- Change in *EnergyTake* due to water draw events.
- Heating sources switching (fan, compressor, and resistive heating element).
- Coefficient of Performance (COP)
- HPWH behavior and ambient temperature.

As mentioned in Section 3.2.1, the DCS sends a *commodity read* query to the water heater every minute. Consequently, the received data is logged by the DCS in a CSV file. The *EnergyTake* is among the reported data. The *EnergyTake* is the amount of energy that the HPWH would need to consume to heat the water in its tank to the temperature set points. For this work, the HPWH set point is set to $120°F$.

3.4.1 Idle Losses

Idle losses is the amount of energy that the device loses over time. The HPWH resides in a lab where the average ambient temperature is $\approx 73°F$. Prior to modeling the device idle losses, the HPWH was fully heated by sending a *load up* command. Once the *EnergyTake* reached 0, indicating the water temperature is equal to the HPWH set point $(120°F)$, a *grid emergency* command was sent to the HPWH to force it to cool down over the course of approximately three days. Given the temperature difference between the HPWH tank and its surroundings, heat is expected to be transferred towards the colder region as per convective heat transfer.

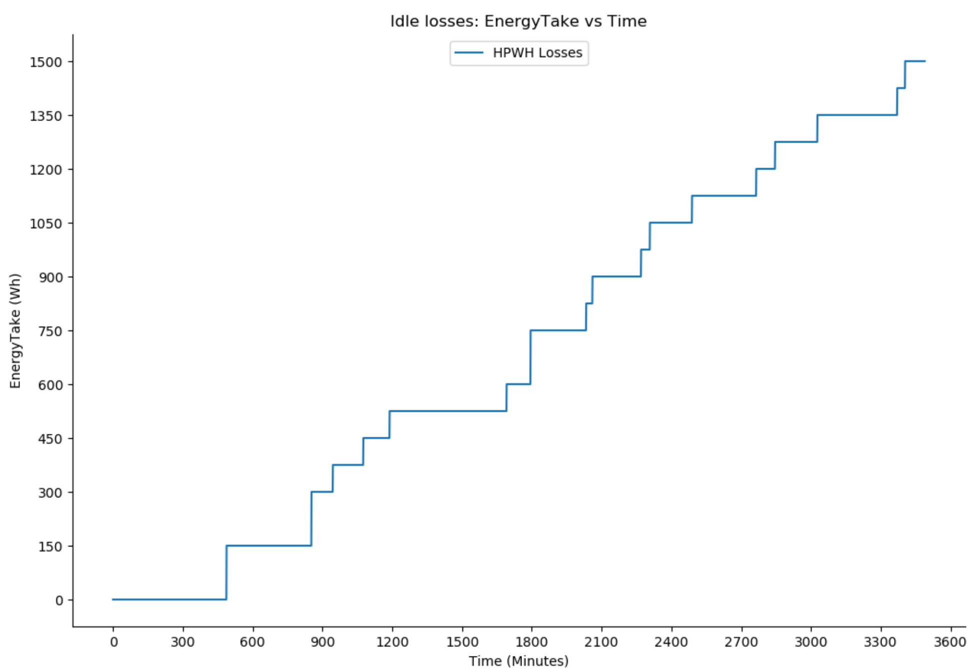

Figure 3.5: HPWH Idle Losses: EnergyTake VS Time

Initially, the cooling process was implemented by setting the HPWH to "vacation mode". However, by design, the HPWH automatically disable the "Grid Enable" mode and, therefore, does not report data when in "vacation mode". Figure 3.5 shows the *EnergyTake* gradually increase over time due to idle losses. Note that the HPWH reports *EnergyTake* in 75 Wh increments. The relationship between the *EnergyTake* and elapsed time is determined using a curve fit function in Python. The equation for this curve is as follows:

$$E(t) = 0.8960 \times t + 126 \tag{3.1}$$

3.4.2 *EnergyTake* and Water Draw Events

Once a water draw occurs, the *EnergyTake* increases rapidly as hot water leaves the tank and cold, influx water replaces it. The heat transfer between the cold and hot water is conserved; the lost and gained heat are shown in equations 3.2 and 3.3.

$$Q_{lost} = V_{WaterTank} \times \rho_{water} \times C_p \times (T_{Setpoint} - T_{mixed\_water}) \tag{3.2}$$

$$Q_{gain} = V_{WaterTank} \times \rho_{water} \times C_p \times (T_{mixed\_water} - T_{inlet}) \tag{3.3}$$

Where

Q_{lost} = Heat lost from the hot water portion within the tank [BTU]

Q_{gain} = Heat gained from the cold water portion within the tank [BTU]

$V_{WaterTank}$ = Volume of the water left the tank after the draw [gpm]

ρ_{water} = Water density $[\frac{\text{lb}}{\text{gal}}]$

C_p = Specific heat of water $[\frac{\text{Btu}}{\text{lb} \cdot \text{F}}]$

T_{inlet} = influx water at $60°F$

The temperature of the mixed water is derived from the above two equations and shown as follows:

$$T_{mixed\_water} = \frac{(V_{WaterTank} \times T_{SetPoint}) + (V_{Draw} \times T_{inlet})}{V_{WaterTank} + V_{WaterDraw}} \tag{3.4}$$

The T_{mixed_water} from equation 3.4 serves as the initial temperature after the water draw occurs. Since the decrease in the water temperature does not happen instantaneously, a ramp rate was added to Equation 3.4. The ramp rate was identified from the physical HPWH unit in the lab. Several water draw events were implemented, where random water draw events ranging from 5 gpm to 25 gpm were scheduled using the DCS. The aforementioned equations were validated against a test case and the results are shown in Section 3.5.

3.4.3 Heating Sources Switching

The heating sources triggering is dependant on the detected *EnergyTake*. The resistive heating element triggers once the *EnergyTake* reaches 2000 Wh and heats the water, though not all the way to the set point. Once the *EnergyTake* drops to 1000 Wh, the resistive heating element turns off, the compressor triggers and then heats the water to the specified set point. Table 3.1 shows the maximum and minimum threshold for each heating source. Note that this process only occurs when an excessive water draw causes this significant rise in the *EnergyTake*.

Heating Source	Threshold Range (Wh)
Resistive Heating Element	2000 - 1000
Compressor	1000 - 0

Table 3.1: Heating Sources Maximum/Minimum Thresholds

Upon observations, it was found that the process that the HPWH follows before triggering a heating source is consistent, regardless of the volume of the water draw event. During normal operations, the thermostat dead-band for the compressor is 675 Wh (equivalent to 115°F). Once the *EnergyTake* hits 675 Wh, the fan turns on for one minute, then the compressor triggers to heat the water. This process is repeated with the resistive heating element as well. Modeling this dynamic is important for DR applications as the delay may exacerbate problems in frequency response services, for instance. Therefore, a "turn_fan_on" variable was set to trigger as the given set point is reached. The rated current for the fan is 0.17 A, resulting in 41 W when connected to a 240 V line.

3.4.3.1 Heating

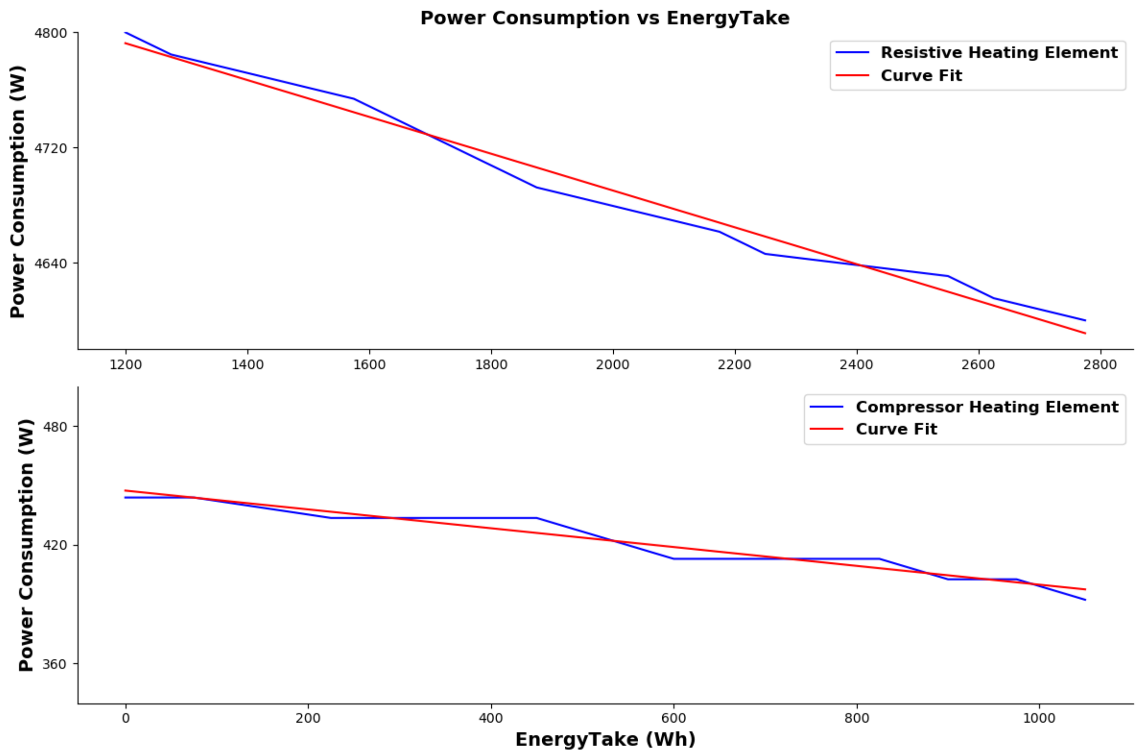

Figure 3.6: HPWH Heating Elements: Power Consumption VS EnergyTake

To determine the heating rate for each heating source, four water draw events were scheduled using the DCS, descending from 30 gpm to 17 gpm. The HPWH was allowed to recover between each water draw event. High volume water draw events were intentionally chosen to ensure that the resistive heating element operated. Figure 3.6 shows the heating process of the resistive heating element (top) and the compressor heating element (bottom). Note that in the top plot, the compressor works with the resistive heating element. A curve fit to the resistive heating element and compressor results in equations 3.5 and 3.6, respectively.

$$P(ET) = 4782 - 0.0014 \times ET \tag{3.5}$$

$$P(ET) = 447.3 - 0.0047 \times ET \tag{3.6}$$

Where

$P =$ Power consumption in Watts [W]

$ET =$ *EnergyTake* in Watts-Hour [Wh]

3.4.4 Coefficient of Performance

The COP is the ratio between the transferred energy to the tank and the consumed energy. While EWHs have an efficiency of one (100%), HPWHs can easily achieve a COP of 2 (200%). NREL conducted a study on three different HPWH brands, and the average range COP for all three units was 1.5 - 2.6. The low COP is mainly caused by the low ambient temperature. A large water draw can trigger the resistive heating element more frequently, which impacts the overall efficiency of the HPWH.

As shown in Figure 3.6, the compressor plot, the relationship between the consumed energy and the *EnergyTake* is linear, where the compressor energy increases as the tank temperature increases. Therefore, the COP is calculated as follows:

$$COP = \frac{Q_{added}}{E_{consumed}} \tag{3.7}$$

Where

$$Q_{added} = ET_{previous} - ET_{current} \qquad [\text{Wh}] \qquad (3.8a)$$

$$E_{consumed} = \int_{t_0}^{t_i} P(t)dt \qquad [\text{Wh}] \qquad (3.8b)$$

To test the COP, the HPWH was set to “Grid Emergency” mode and the DCS was used to monitor the *EnergyTake*. Once the *EnergyTake* reached 2000 Wh, the DCS would send a *load up* command to heat the water by triggering only the compressor. As shown in Figure 3.7, the COP ranges between 2.3 and 2.9 while the compressor heats the water to the specified set point.

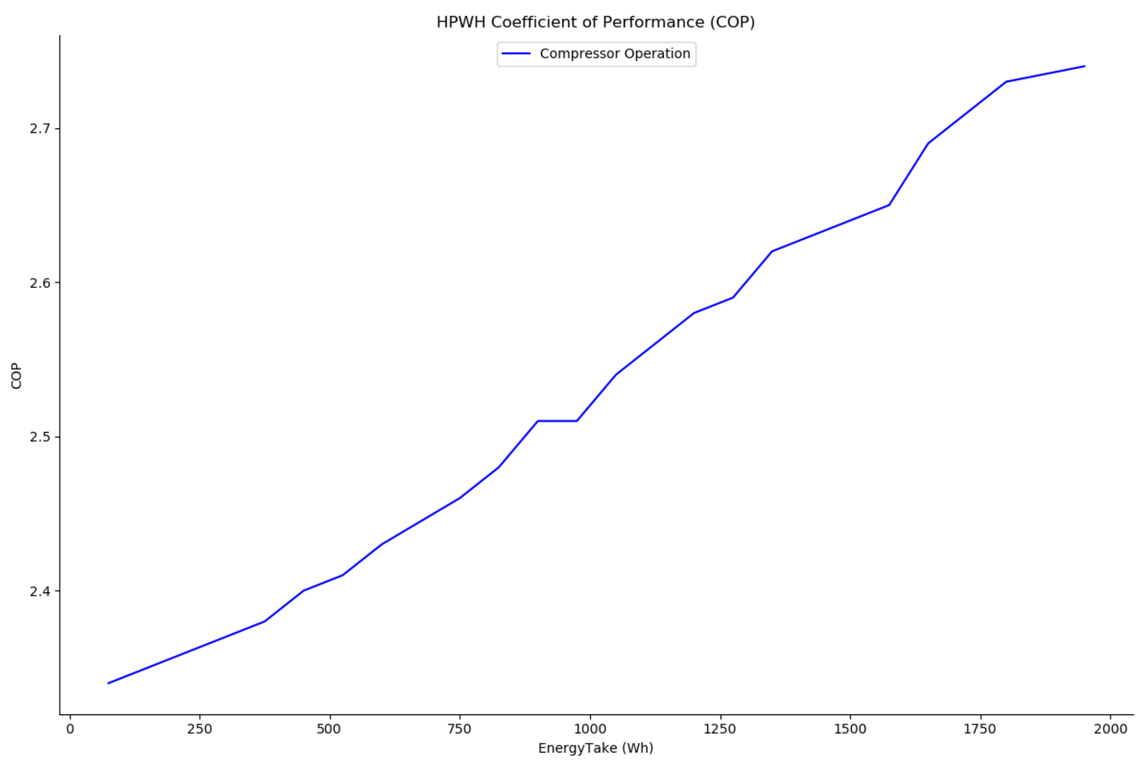

Figure 3.7: HPWH COP VS EnergyTake

3.4.5 HPWH and Ambient Temperature

The ambient temperature in the space surrounding the physical HPWH unit used in this thesis work is approximately 73°F. The previously mentioned NREL study, which included three different HPWH brands, reported that one particular HPWH unit had lower than average COP due to cold ambient temperatures (50°F - 60°F) [19]. Such temperature conditions increase idle losses of HPWHs and reduce their recovery rate. Consequently, forcing HPWHs to trigger the resistive heating elements more frequently than the compressor. Given that the change in ambient temperature impacts the HPWH performance significantly [15], it is imperative to evaluate the HPWH model behavior over various ambient temperature values. This Subsection presents the methods used to analyze the ambient temperature impact on the developed HPWH model in GridLAB-D. Further, it compares its performance under two ambient temperature values, 60°F and 73°.

Performing such a test requires moving the physical HPWH unit to another lower ambient temperature location or adjusting the current working environment temperature. Both of these solutions are expensive and labor intensive. Therefore, the behavior of the developed HPWH model behavior in cold surrounding space was an estimation of the results presented in this work [19]. The two dynamics considered while modeling the behavior of the HPWH in 60°F environment are as follows:

- Idle losses.
- Heating sources operation.

3.4.5.1 Idle Losses at 60 °F and 73 °F

GridLAB-D provides a *climate* module that retrieves climate data from TMY files. The TMY files contain aggregated and averaged weather data for a particular geographical location that is specified in the GLM file [32]. *House* and *water heater* objects, for instance, interface with the *climate* module to account for the ambient temperature in their calculations. Within the *residential* module source code, where *house* and *water heater* objects reside, a "get_Tambient(location)" function is defined that returns the average ambient temperature associated with the specified location. For this test, the "get_Tambient(location)" function was set to return average ambient temperature of 60 °F.

To test the developed HPWH model behavior in a colder ambient temperature, the type of the water heater object was set to "HEAT_PUMP". The tank was allowed to sit idle with no water draw events scheduled during the idle period. The other parameters, including tank set-point and tank size, remained the same as all the tests in this thesis work. Figure 3.8 illustrates the idle period, where the tank begins fully charged and reheats once the minimum tank set-point is reached at the end of the idle period. During the idle period, the tank temperature decreases over a 23 hours period before reaching the minimum set-point threshold in a 73 °F ambient temperature environment. This behavior corresponds to the physical HPWH unit that resides at PSU, in the PowerLab. At 60 °F ambient temperature, however, the tank loses heat at a faster rate due to the increased difference between the tank temperature and the ambient temperature. Note that the tank temperature decreased over the course of 19 hours, approximately four hours less than the HPWH behavior at 73°F ambient temperature. Furthermore, the compressor heating period for both cases is different. In the first case, where the ambient temperature was set to 73 °F, the compressor takes ≈ 44 minutes to heat the water to the tank set-point. In the second case, where the ambient temperature was set to 60 °F, the compressor takes ≈ 75 minutes to heat the water to the tank set-point.

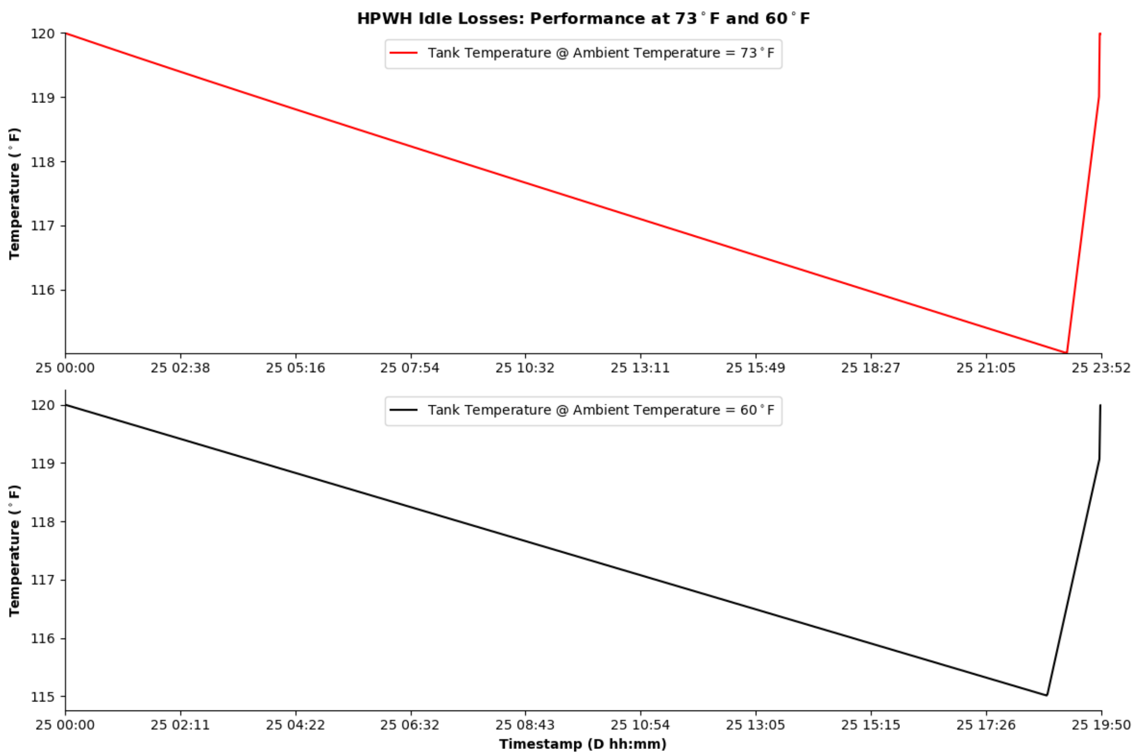

Figure 3.8: HPWH Idle Losses: Tank Temperature Behavior at 60 °F and 73 °F

3.4.5.2 Heating Sources at 60 °F and 73 °F

To test the behavior of the heating sources in 60 °F and 73 °F ambient temperatures, the HPWH was set to draw 20, 15, and 10 Gallon Per Minute (GPM) water draw events at three different times. After each water draw event, the HPWH model was allowed to recover and heat the water to the tank set-point. Figure 3.9 depicts the heating sources responses to the drop in tank temperature due the three water draw events at 60 °F and 73°F ambient temperatures. Note that in the first and second water draw events at 60°F, the 20 GPM and 15 GPM, the resistive heating element was triggered to heat the water. However, the same water draw events triggered only the compressor at 73°F. Such behavior is expected for the following reason. Since the HPWH loses heat at a faster rate in cold spaces, even the relatively small water draw events causes the HPWH temperature to drop below the minimum threshold for the resistive heating element. Even though the resistive heating element did not trigger in the last water draw event, the 10 GPM, the compressor spent more time to heat the water to the tank set-point. In the 73 °F ambient temperature environment, the compressor heated the water for 94 minutes. However, in the 60 °F ambient temperature environment, the compressor spent 153 minutes to heat the water to the tank set-point.

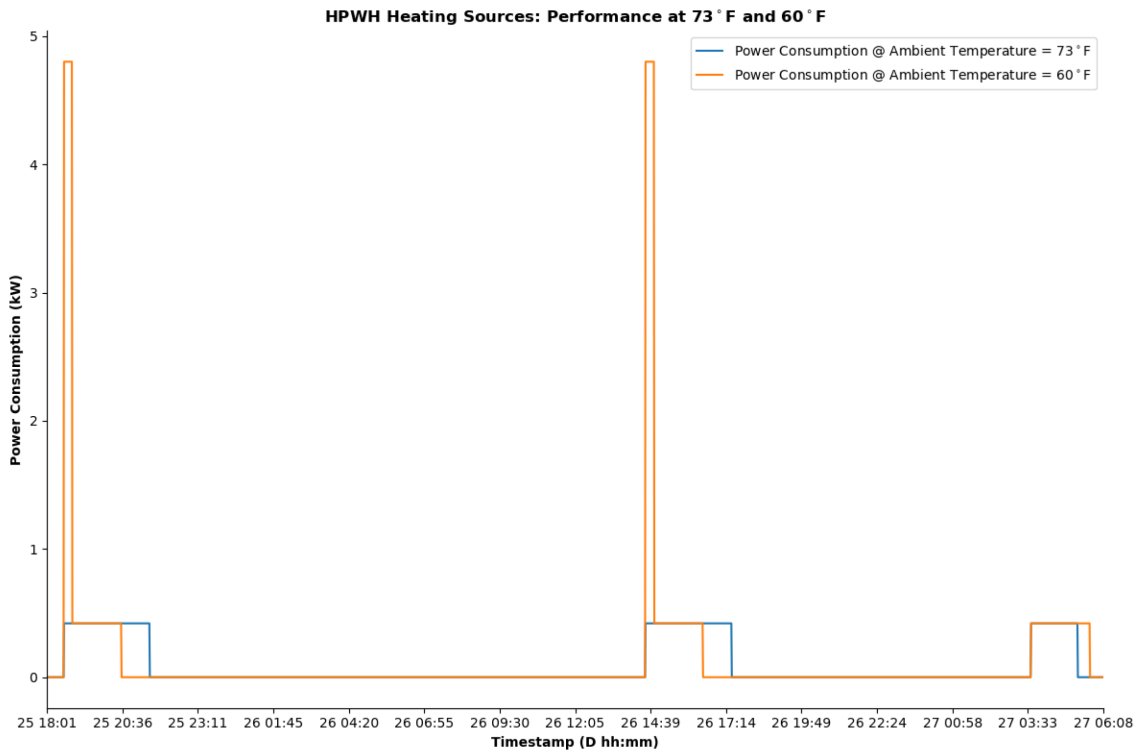

Figure 3.9: HPWH Heating Sources: Power Consumption Behavior at 60 °F and 73 °F

3.5 Heat Pump Water Heater Validation

The physical HPWH unit used to develop the HPWH model in this work was used in a collaboration project between PSU and PGE [9]. The project, referred to as the Energy Management Circuit Breaker (EMCB) project hereafter, investigates the issues associated with DLC method to control water heaters, where several water draw schedules and load shifting scenarios were applied.

The validation process addresses the following three main dynamics to ensure accuracy and efficiency:

- HPWH heating sources switching.

- HPWH temperature representation.
- HPWH idle losses.

3.5.1 Heating Sources Switching

The EMCB project investigated three water draw events, as shown in Table 3.2. These water draw events constitute the basis of the validation testing procedure. To test the heating sources switching, both the GridLAB-D model and the physical HPWH were set to run the first water draw event, the 20 gpm. The output data were then plotted alongside each other for analysis.

Figure 3.10 shows the behavior of the physical unit and the developed HPWH model. As mentioned in Section 3.4.3, the HPWH detects the increase in the *EnergyTake*, then operates the needed heating source. In this test, the HPWH controller detected a large increase in the *EnergyTake* ($\geq$ 2000 Wh) due to the 20 gpm water draw event. Therefore, the fan triggered for one minute, then the resistive heating element triggered. Because the fan consumes 41 W, an insignificant small portion compared to the resistive heating element, an embedded figure was created to illustrate the fan operation. Once the *EnergyTake* dropped below the minimum resistive heating element threshold, 1000 Wh, the resistive heating switched off, thereby triggering the compressor to heat the water to the specified set point.

Event	Time	Amount
Morning Shower	6:45 a.m.	20 Gallons
Dish Washer	7:00 p.m.	5 Gallons
Evening Shower	8:00 p.m.	10 Gallons

Table 3.2: Automated water draw schedule [9]

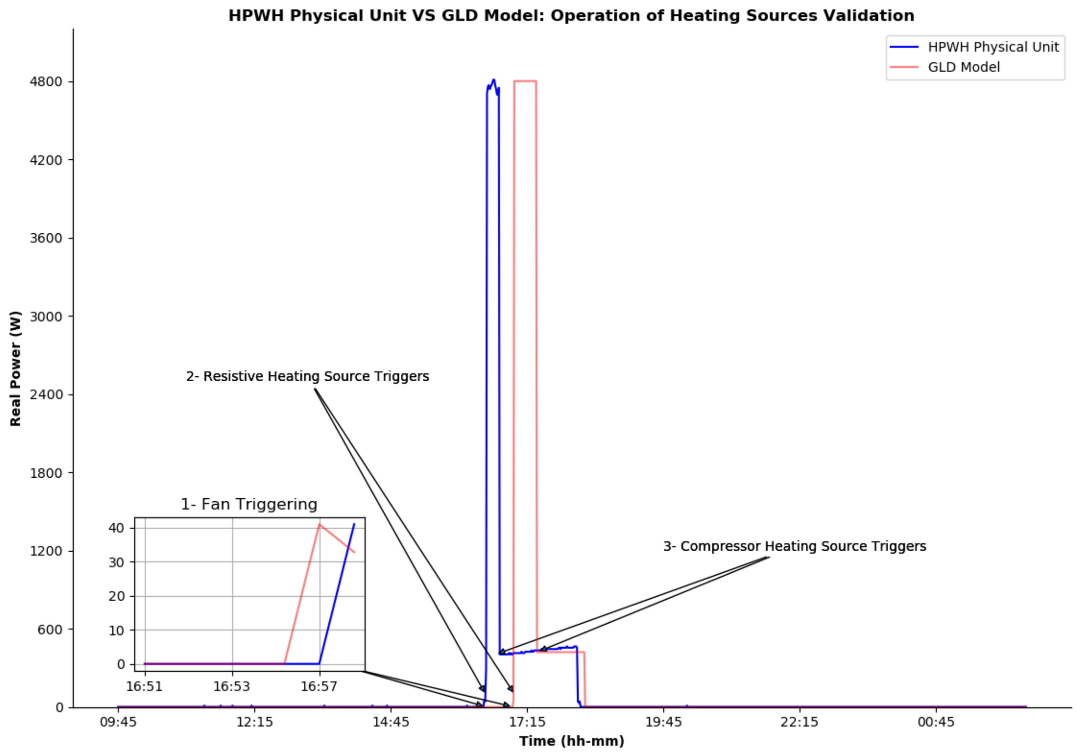

Figure 3.10: Water Draw Validation: HPWH Physical Unit VS HPWH GLD Model

3.5.2 Heat Pump Water Heater Model Temperature Representation

The physical HPWH unit reports *EnergyTake* that represents the average tank temperature. Because the *EnergyTake* is a novel metric pioneered by EPRI [33], a “temperature” variable was used instead of the *EnergyTake* while developing the HPWH model. As a water draw event occurs, the HPWH calculates the initial temperature drop within the tank as shown in Section 3.4.2, then converts it to *EnergyTake* to start the heating process.

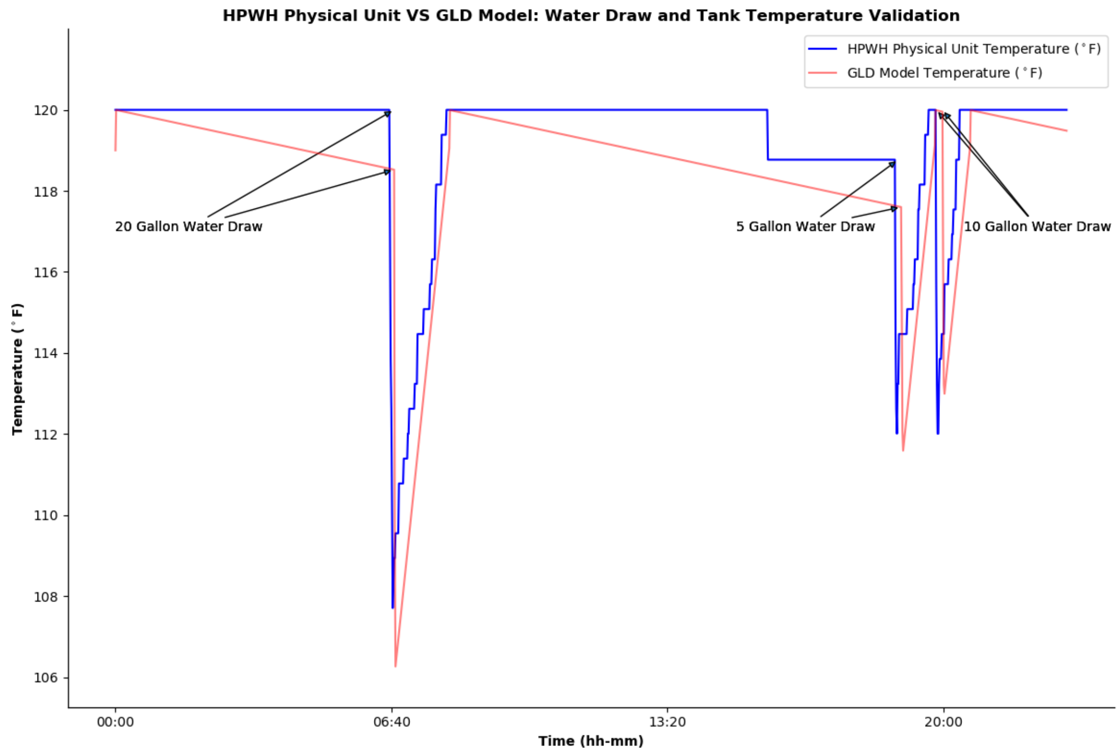

Figure 3.11: Temperature Validation: HPWH Physical Unit VS HPWH GLD Model

For this test, all water draw events shown in Table 3.2 were applied in the GridLAB-D HPWH model. The results were then compared with the EMCB project data. Figure 3.11 shows the water temperature change due several water draw events. Unlike the HPWH model, the temperature variation of the physical unit is minimal. This is due to the fact that the physical HPWH unit reports *EnergyTake* in 75 Wh increment. Further, this factor affected the data correlation as well. A Python function determined that the Normalized Root Mean Square Error (NRMSE) is $\approx 74\%$.

3.5.3 Idle Losses Validation Test

The idle losses validation test was implemented by setting the HPWH physical unit in idle mode. Neither CTA-2045 commands nor water draw events were used. By design, the HPWH thermostat dead-band is set to $5°F$. Accordingly, the GridLAB-D HPWH model was set to the same thermostat dead-band.

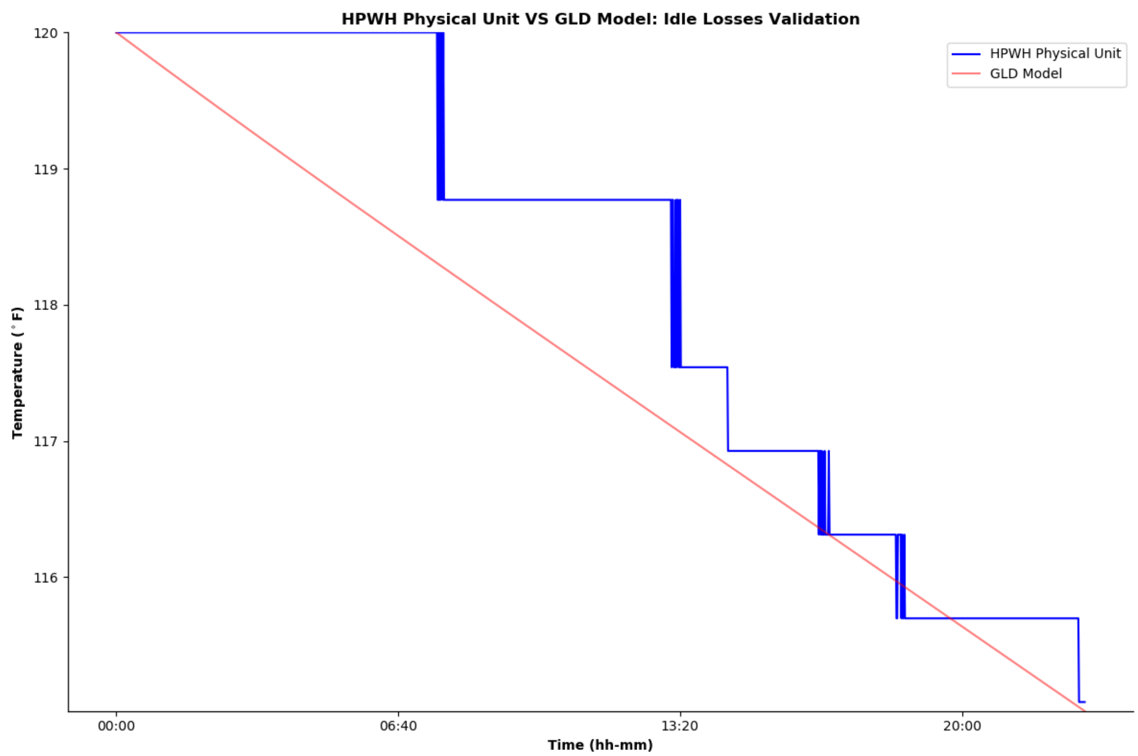

Figure 3.12: Idle Losses Validation: HPWH Physical Unit VS HPWH GLD Model

While conducting the EMCB study, it was noted that the HPWH losses thermal energy relatively slower than the EWH. As reported by Clarke [3], this might be due to the fact that there is incidental thermal insulation provided by the condenser coils that are wrapped around the tank within the HPWH. Regardless, the aspect was also considered while developing the GridLAB-D HPWH model as shown 3.12.

3.6 IEEE-13 Node Test Feeder

The IEEE 13 Node Feeder used for this work was inherited from S. Alomani [23]. Nevertheless, the designated household profiles used for the current work are not the same, thereby requiring different specifications for some system components such as distribution transformers. The simulation time and load distribution were not changed. This Section focuses on the differences between the inherited model and the current model, and illustrates the significance of the changes made to achieve the goals of the work presented here.

The selected feeder to evaluate the impact of HPWHs penetration on distribution systems is the IEEE 13 Node Test Feeder, shown in Figure 3.13. The IEEE 13 Node test Feeder is a radial system with a nominal voltage of 4.16 kV. This feeder comprises several distribution system components, including substation transformers, distribution transformers, overhead and underground lines, voltage regulators, and capacitor banks.

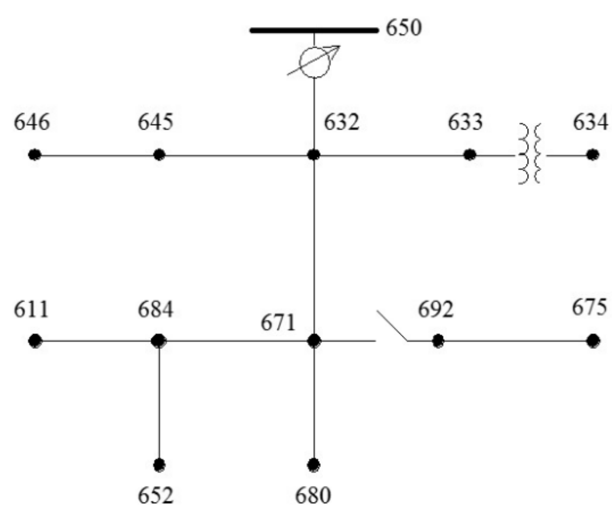

Figure 3.13: IEEE 13 Node Test Feeder One-line Diagram [34]

3.6.1 Feeder Configuration

Generally, a distribution system scheme facilitates a split-phase level system that mainly uses two-phase rather than three-phase configuration. This is the scheme in typical houses in the United States as they are configured with 120/240 V panels to accommodate various end-use loads within the house. GridLAB-D represents such paradigm with *triplex* objects. The *triplex* objects require its linked components to be of *triplex* type as well. Accordingly, the original 13 Node Test Feeder model was adjusted to serve $\approx$ 1000 loads by adding *triplex* objects to each node, shown Figure 3.14.

Figure 3.15 shows the components of the *triplex* system. The split-phase transformer facilitates the "link" between the three-phase and the two-phase systems. It steps down the voltage for each phase to 120 V. The *triplex Node* object facilitates a connection point, where several end-use loads may be attached to it. In this work, the end-use loads are simulated as a "*Triplex load*" object and a "water heater" object. The "*triplex load*" object was used to mimic a typical household demand profile. The *water heater* object, on the other hand, has an attribute that allows users to define its type. In this work, "Electric" and "HEAT_PUMP" were used alternatively.

3.6.2 End-use Loads Configuration

Though the feeder incorporates 13 nodes, two nodes were neglected while configuring the model to accommodate the end-use loads. First, node *650* is of "Swing" bus type. The "Swing" bus is used to facilitate system losses when absorbing or providing reactive power.

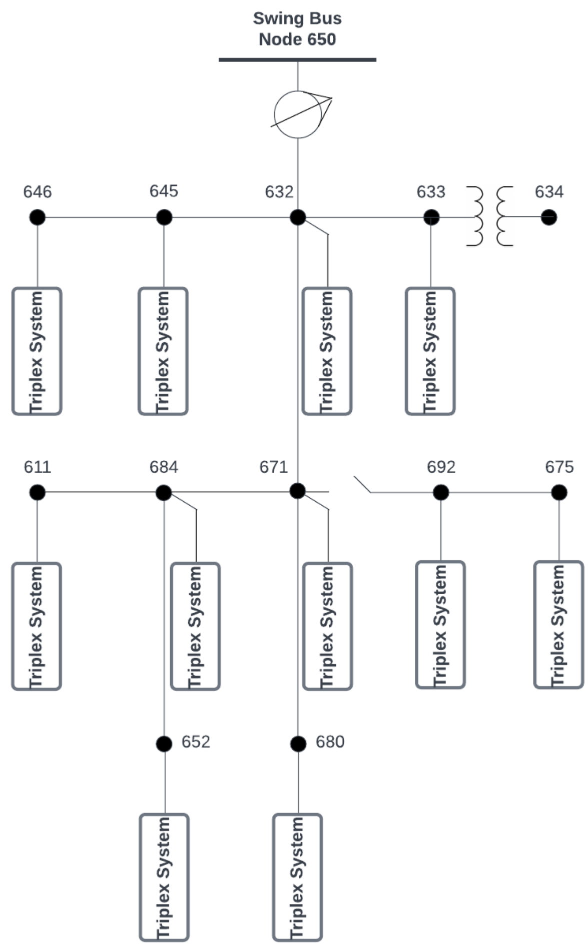

Figure 3.14: Modified IEEE 13 Node Test Feeder Model

Second, Node *634* is linked to a substation transformer that is configured as 3ϕ, 480 V. As such, these two nodes were not considered in this work, as they were designated for high voltage loads such as level 3 EV chargers [23].

While the load distribution remained the same as in [23], the transformer ratings were adjusted accordingly to accommodate the household demand profiles. The household demand profiles were obtained from the Northwest Energy Efficiency Alliance (NEEA) Residential Building Stock Assessment (RBSA) metering study [35]. The metering study

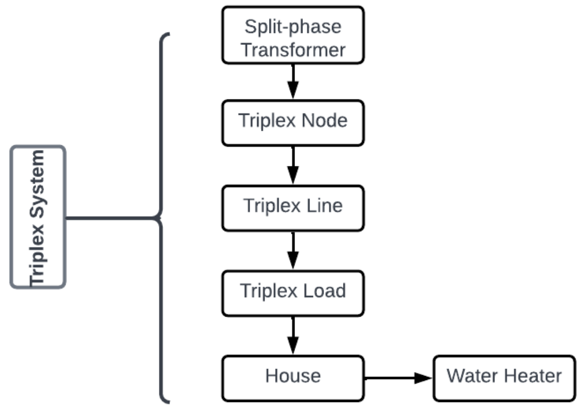

Figure 3.15: Triplex System Components

focused on a variety of residential end-use loads, including lighting, house appliances, EVs, and hot/cold water draws. The study was designed to represent a single-family house across the Pacific Northwest for 27 months. The uniqueness of this dataset is that it illustrates each end-use load individually. This is helpful to this work as the water heater, and the house models are two individual objects. To avoid duplicated data, the water heater demand profiles within the RBSA dataset were excluded from the house demand profiles.

Several measures were taken to ensure diversity and consistency between all the case studies. These measures are identified within the used demand profiles and the end-use loads' configurations. As reported by U.S Census Bureau, the average number of bedrooms in a single-family household is shown in Table 3.3. Therefore, the house demand and water draw profiles identified are the two, three, and four bedrooms. These profiles were then randomly distributed over the 1000 loads within the feeder model.

The water heater behavior, on the other hand, is diversified as much as their water draw profiles. However, the water heaters size, set-points, and thermostat dead-band may increase

Number of Bedrooms	Percentage
One	11%
Two	25%
Three	39%
Four or more	17%
Five or more	4.6%

Table 3.3: Average Household Number of Bedrooms in a Single-Family House [36]

idle losses and heating periods. Therefore, some assumptions were made while developing the case studies for this work. These assumptions correspond to the water heater tank characteristics. For instance, a water heater object in this thesis is configured as follows:

```
object waterheater {
    name wh1;
    location INSIDE;
    temperature 120.0;
    thermosat_deadband 5.0;
    inlet_water_temperature 60.0;
    tank_setpoint 120.0;
    tank_volume 50.0;
    water_demand wd.value;
    heat_mode Electric;
    object player {
        name wd;
        file "wd_1.csv";
        };
    }
```

The water temperature, tank set_point, thermostat_deadband, and tank_volume attributes were set the same for all case studies to ensure simulation consistency. In other words, water heaters are assumed to be initially fully charged, where the water temperature is equal to the set point ($120°F$). Note that the "heat_mode" attribute was used interchangeably to indicate the water heater type, whether an EWH or a HPWH. Further, the "water_demand" attribute is assigned an object name, called *player* object. The *player* object reads the water demand profile and assigns each value, with its corresponding timestamp, to the "water_demand" attribute.

4 Results & Discussion

The goal of this work is to evaluate the impact of HPWH deployment on distribution systems. Because HPWHs are projected to be the majority of water heating systems used within the residential sector by 2039 [37], five case studies were developed to investigate their impact on distribution systems. Initially, all houses within the feeder model were deployed with EWHs devices. The penetration of HPWHs was then incremented by 20% where EWHs are replaced with HPWHs with the same characteristics. The energy consumption and peak demand are evaluated in each case. The expected outcome for each case study is to observe less energy consumption and, consequently, a reduction in the peak demand as HPWHs penetration level increases.

4.1 Base Case

The IEEE 13 Node Test Feeder comprises 13 nodes. For this work, a single-phase, two-phase, and three-phase nodes are illustrated, shown in Appendices A and B. In order to attain detailed results for the base case, node 633 was chosen as it facilitates three phases. In each phase, five *distribution transformer* objects were deployed. Consequently, eight end-use loads were attached to each transformer, resulting in 40 end-use loads per phase and 120 end-use loads in node 633.

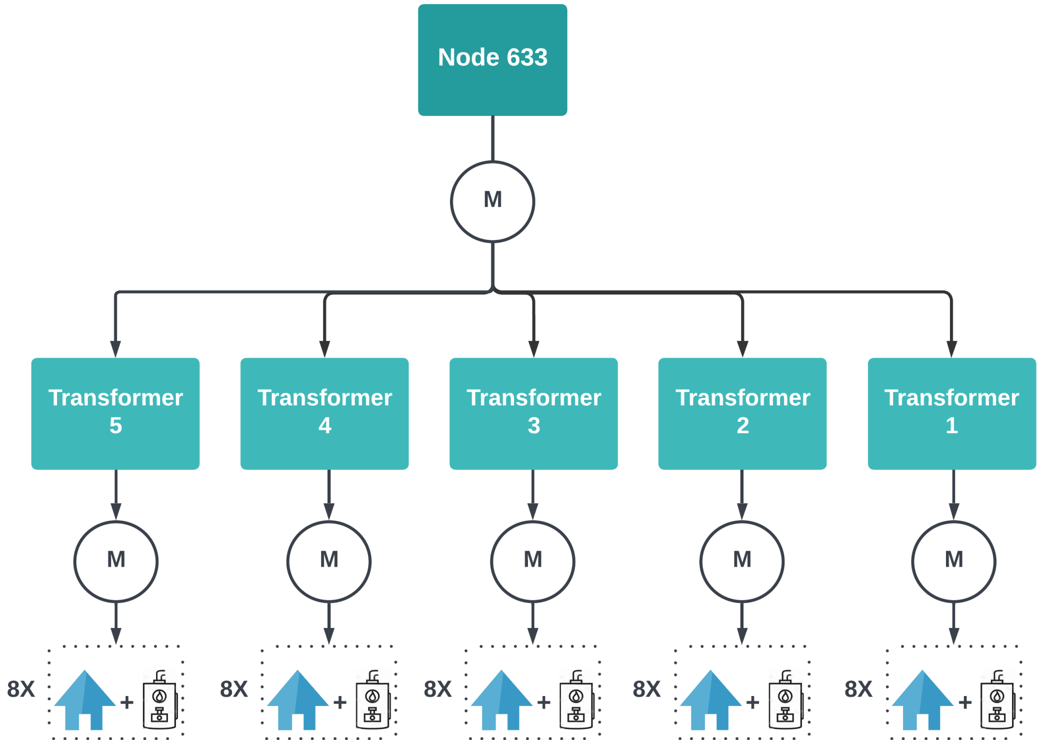

Figure 4.1: Node 633 in IEEE 13 Node Test Feeder

The base case depicts the behavior of the distribution system with the absence of HPWHs. As mentioned previously in Section 3.6.1, a *distribution transformer* object is used to link the three-phase system with the triplex system. Figure 4.1 shows the structure of end-use loads in each phase in node 633 in the IEEE-13 Node Feeder. The end-use loads are simulated in the *triplex load* objects and *water heater* objects. The *triplex load* objects are used to simulate a single-family household demand profile, where each object reads a distinctive demand profile in kW. Similarly, each water heater object reads a distinctive water demand profile. Figures 4.2 - 4.3 show samples of the water draw profile (GPM) and household demand profile (kW), respectively.

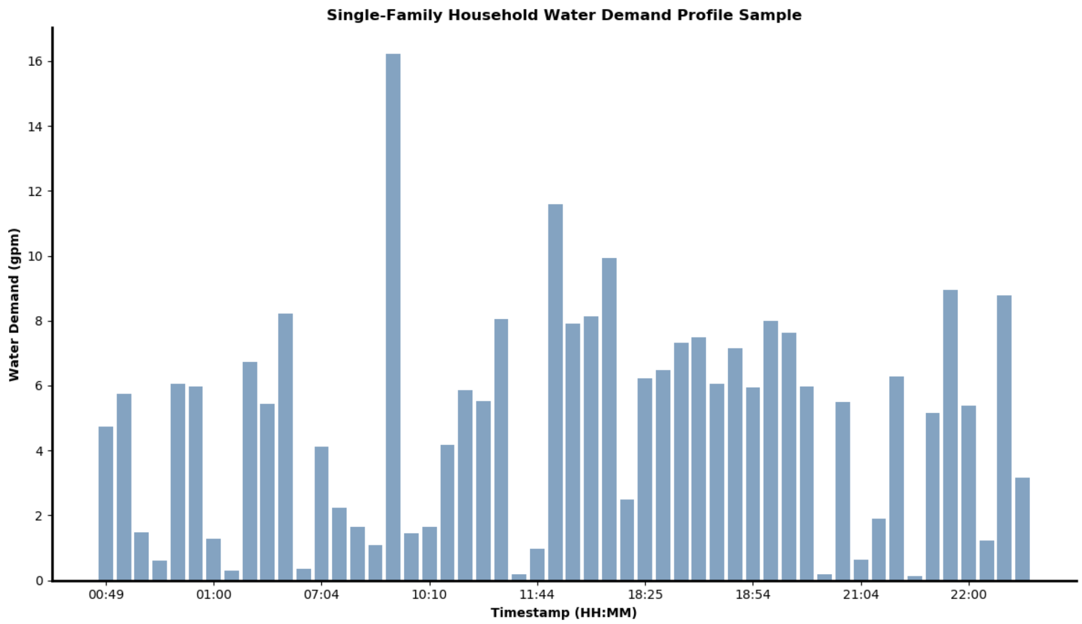

Figure 4.2: A Sample of Water Draw Profiles Used in *Water Heater* Objects

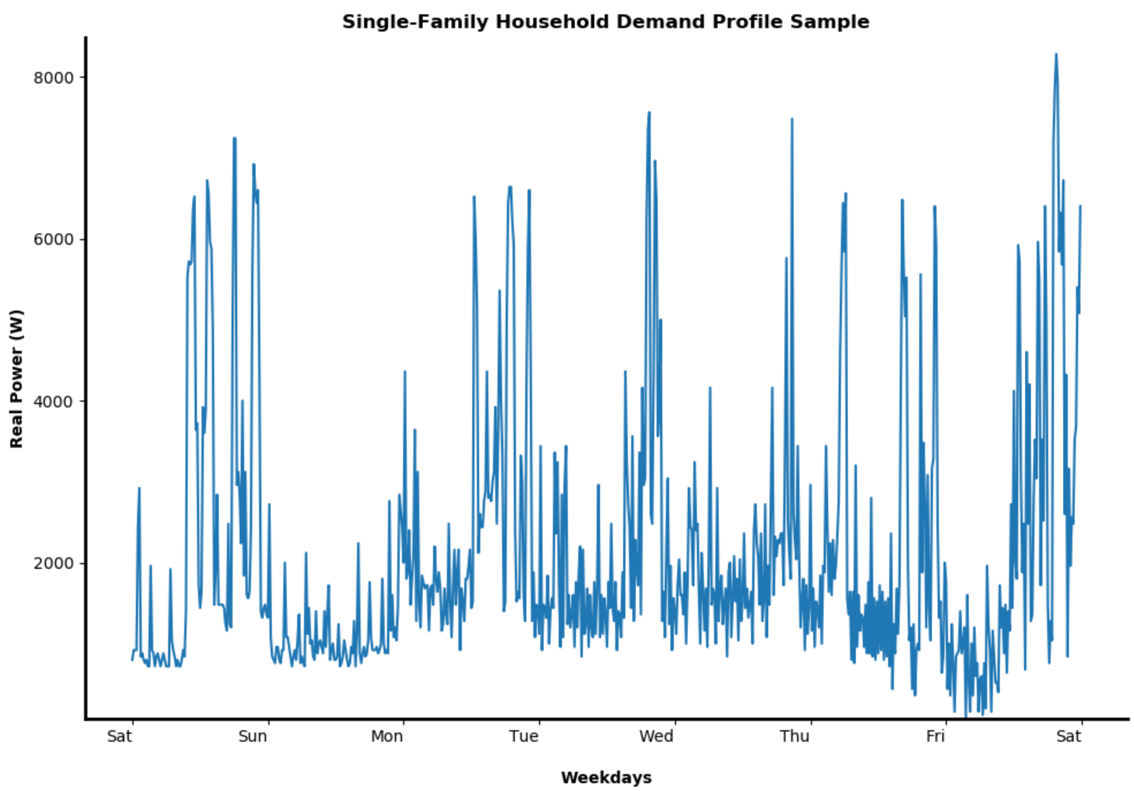

Figure 4.3: A Sample of a Single-Family Household Demand Profile Used in *Triplex Load* Objects

All the *water heater* objects are of EWH type in the Base case. Figure 4.4 depicts the delivered apparent power in kVA by the five transformers in each phase. One can observe that the peak demand reached 207 kVA in phase A, 150 kVA in phase B, and 145 kVA in phase C for the base case. Further, the energy consumption of the houses and the EWHs in phase A is recorded as 122 kWh and 92 kWh for phases B and C.

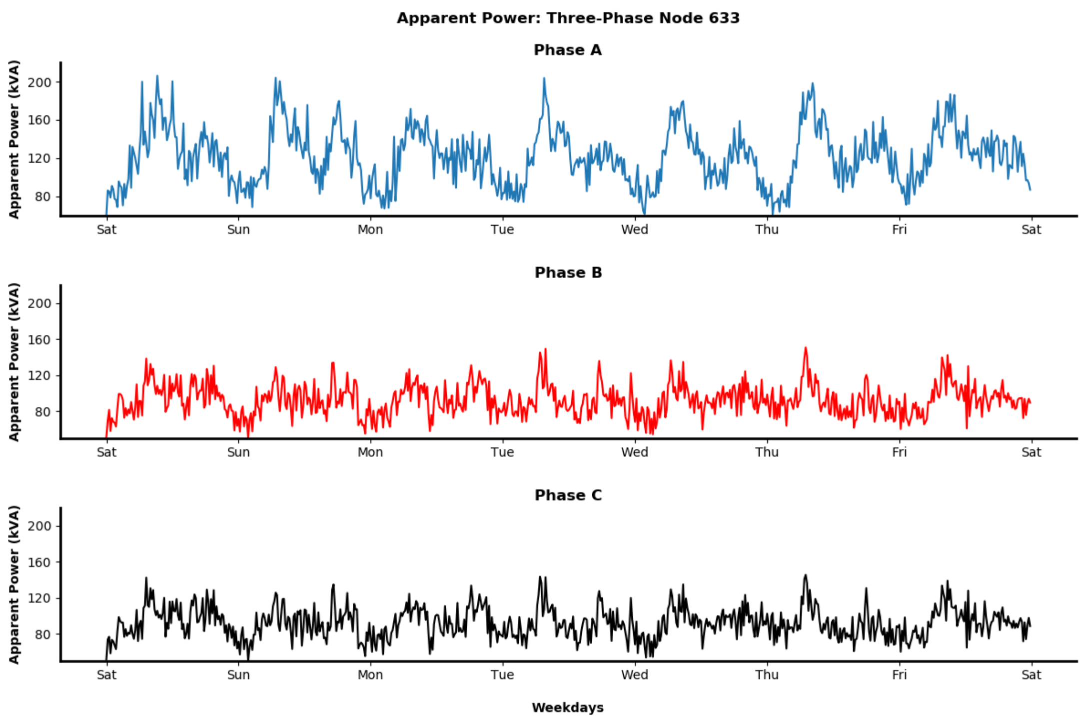

Figure 4.4: Base Case: The Distribution Transformer Delivered Apparent Power Data in kVA for Node 633

4.2 HPWH Case Studies

The HPWH case studies are developed to investigate HPWH impact on distribution systems. The analysis of the HPWH case studies includes five cases. In each case, 20% increments of HPWHs penetration are deployed in each node, where EWHs are replaced with the developed HPWH model. The tank characteristics, water draw profiles, and household demand profiles remain the same as the Base case to ensure accurate and consistent results. A comparison between the Base case and each HPWH case is discussed. The data presented in this Section are associated with the 80% and 100% HPWH penetrations. The rest of the simulated cases are shown in Appendix B. Like the Base case study, node 633 was chosen for analysis purposes.

4.2.1 80% Heat Pump Water Heater Case Study

In this case study, 80% of the EWHs objects within node 633 were replaced with HPWHs. The 80% HPWH penetration case constitutes 96 HPWHs and 24 EWHs objects. The delivered apparent power by the distribution transformers in kVA was recorded by their associated meters. Figure 4.5 illustrates the delivered apparent power of the Base case and the 80% penetration case study. The peak demand for phases A, B, and C reached 175 kVA, 116 kVA, and 133 kVA, respectively, for the 80% HPWH penetration case. Compared to the Base case in Section 4.1, the peak demand is mitigated by 13% for phase A, 23% for phase B, and 8% for phase C. Further, the energy consumption (kWh) in phases A, B, and C were reduced by 25%, 29%, and 10%, respectively.

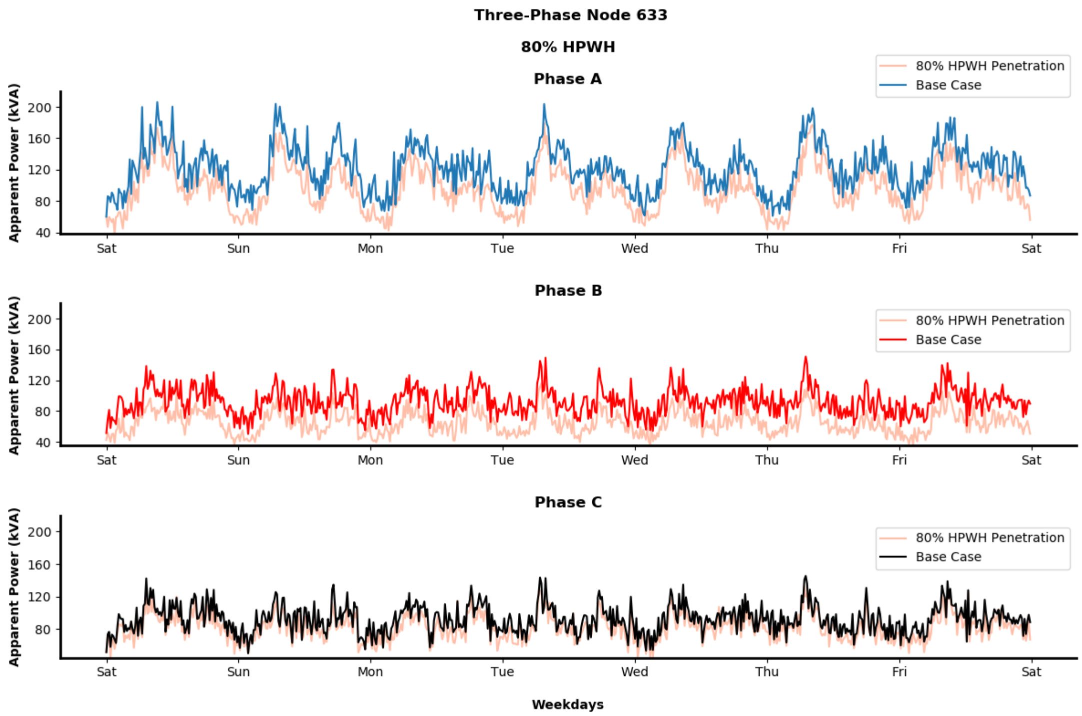

Figure 4.5: 80% HPWH Penetration: The Distribution Transformer Delivered Apparent Power Data in kVA for Node 633

4.2.2 100% Heat Pump Water Heater Case Study

In this case study, all EWHs in node 633 were replaced with HPWHs. The 100% HPWH penetration case includes 120 water heater objects, all of type HPWH. Note that the water draw profiles, household demand profiles, and water heaters characteristics remain the same as the Base case. Figure 4.6 showcases the apparent power data recorded by the meters associated with the five distribution transformers in each phase. Unlike the Base case, the peak demand reported for the 100% HPWH penetration case was recorded as 170 kVA for phase A, 114 kVA for phase B, and 112 kVA for phase C. As such, the peak demand in the 100% HPWH penetration case is reduced by 14% in phase A, 24% in phase B, and 23% in phase C, compared to the Base case. Accordingly, the energy consumption of the end-use loads in kWh was reduced by 26% for phase A and 30% for phases B and C due to the presence of HPWHs.

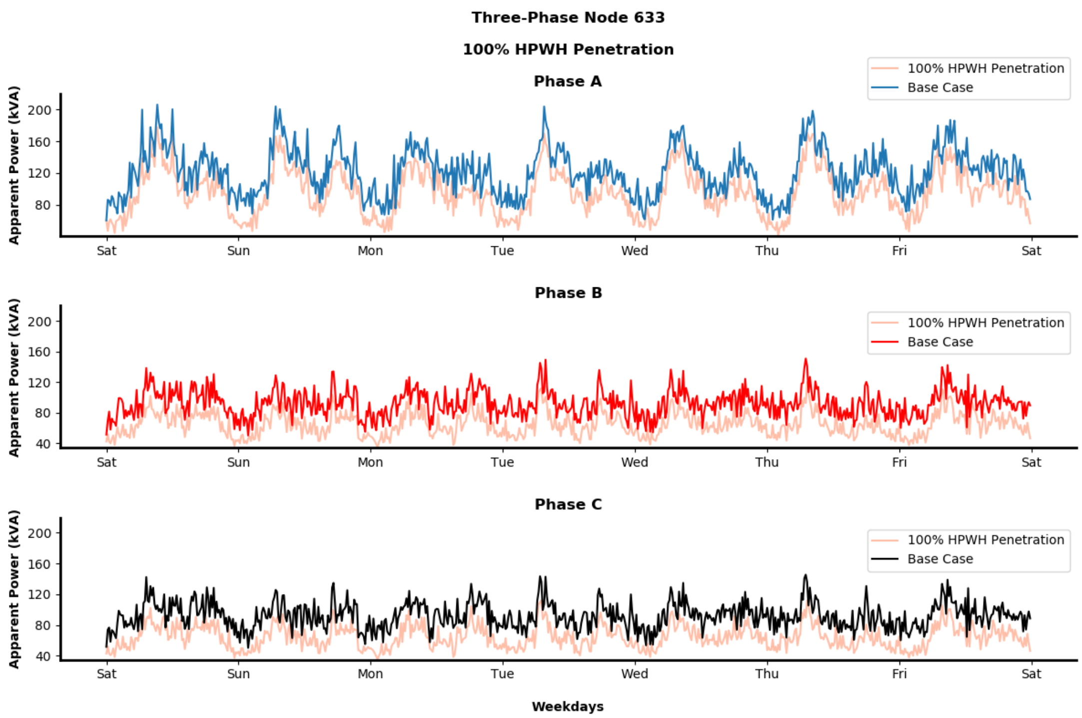

Figure 4.6: 100% HPWH Penetration: The Distribution Transformer Delivered Apparent Power Data in kVA for Node 633

4.2.3 HPWH Case Studies Summary

While increasing the penetration level of HPWHs, it was found that the energy in Wh and the peak load in kVA were significantly reduced. Tables 4.1- 4.2 summarizes the energy reduction (kWh) and peak load mitigation in each HPWH penetration level in node 633.

Table 4.1: Summary of Energy Consumption by End-Use Loads in Node 633

Case Study	Energy Consumption by End-Use Loads (kWh)			Percentage of Energy Consumption by End-Use Loads		
	A	B	C	A	B	C
Base Case	121.6	92.3	92			
20%	105.9	92.1	91.2	14%	1%	0.8%
40%	95.2	87.7	90.4	22%	5%	1.7%
60%	93.1	70.3	87.1	23%	23%	5.4%
80%	90.3	65.7	82.2	25%	29%	10%
100%	89.2	64.8	64.5	26%	30%	30%

Table 4.2: Summary of Peak Load Mitigation in Node 633

Case Study	Peak Load in kVA in Each Phase			Percentage of Peak Load Reduction in Each Phase		
	A	B	C	A	B	C
Base Case	207.1	150.3	145.4			
20%	206.4	149.4	144.7	0.5%	0.7%	0.7%
40%	179.6	146.3	143.7	13%	2.7%	1.2%
60%	179.3	119.1	141.2	13%	21%	2.9%
80%	175.4	116.3	133.4	15%	23%	9%
100%	170.2	114.5	112.7	18%	24%	23%

5 Conclusion

This thesis work successfully modeled and integrated a HPWH model within GridLAB-D simulation environment. By using a real HPWH unit at PSU, the developed model was validated. Further, the model was used in a case study that aims to evaluate the significance of various HPWHs penetration levels in providing reduced peak load.

The case study incorporated five HPWH penetration levels, ranging from 20% to 100%. As HPWH penetration level increases, the peak load (kVA) and the energy consumption (kWh) were reduced. The results showed that a high population of HPWHs can reduce the peak load by 28% and the energy consumption by 38%. As such, HPWHs not only benefit utilities to reduce peak demand, they also help consumers to reduce their overall energy consumption.

The developed HPWH was integrated within GridLAB source code, which is an open-source framework for modeling distribution systems. One can conveniently use the developed HPWH model by assigning the "HEAT_PUMP" value to the "heat_mode" attribute in the water heater object. Such addition expands the utility of the framework to keep pace with the projected HPWH deployment in the future. Once the updated version of GridLAB-D source code is handed to GridLAB-D developers, the HPWH model shall be available in the next release on GitHub.[4]

[4] GridLAB-D Source Code GitHub

This work may be extended to include different types of HPWHs that could be implemented within GridLAB-D simulation environment. The control logic of each unit may be different from one manufacturer to another. For instance, the testing unit used in this thesis is A. O. Smith, which reports *EnergyTake* in 75 Wh increments. Other manufacturers design their HPWH units to report *EnergyTake* at a different rate [17]. Further, the minimum and maximum boundaries of each heating source may also be different. These factors significantly impact HPWHs behavior [19].

Bibliography

[1] Mohammed Yekini Suberu, Mohd Wazir Mustafa, and Nouruddeen Bashir. Energy Storage Systems for Renewable Energy Power Sector Integration and Mitigation of Intermittency. *Renewable and Sustainable Energy Reviews*, 35:499–514, 2014.

[2] U.S. Energy Information Administration EIA Independent Statistics and Analysis. Residential Energy Consumption Survey (RECS). 2020.

[3] T. Clarke. Aggregation of Electric Water Heaters for Peak Shifting and Frequency Response Services. Master's thesis, Portland State University, June 2019.

[4] D. P. Chassin, K. Schneider, and C. Gerkensmeyer. Gridlab-D: An Open-source Power Systems Modeling and Simulation Environment. In *2008 IEEE/PES Transmission and Distribution Conference and Exposition*, pages 1–5, 2008.

[5] M. Albadi and E. El-Saadany. Demand Response in Electricity Markets: An Overview. In *IEEE PES GM*, pages 1–5, 2007.

[6] J. Torriti, M. Hassan, and M. Leach. Demand Response Experience in Europe: Policies, Programmes and Implementation. *Energy*, 35(4):1575–1583, 2010.

[7] M. Obi. *Aggregated Water Heater System Optimization for Ancillary Services*. PhD thesis, Portland State University, April 2020.

[8] Linas Gelazanskas and Kelum A.A. Gamage. Demand Side Management in Smart Grid: A Review and Proposals for Future Direction. *Sustainable Cities and Society*, 11:22–30, 2014.

[9] M. Adham, M. Obi, and R. Bass. A Field Test of Direct Load Control of Water Heaters and its Implications for Consumers. In *IEEE PES GM*, 2022. Accepted for publication.

[10] Karen Stenner, Elisha R. Frederiks, Elizabeth V. Hobman, and Stephanie Cook. Willingness to Participate in Direct Load Control: The Role of Consumer Distrust. *Applied Energy*, 189:76–88, 2017.

[11] J. Stitt. Implementation of a Large-Scale Direct Load Control System-Some Critical Factors. *IEEE Trans. on Power Apparatus & Systems*, 104(7):1663–1669, 1985.

[12] S. Jones. Toward an acceptable definition of service [service-oriented architecture]. *IEEE Software*, 22(3):87–93, 2005.

[13] L. Xu, W. He, and S. Li. Internet of Things in Industries: A Survey. *IEEE Trans. on Ind. Informatics*, 10(4):2233–2243, 2014.

[14] T. Slay and R. Bass. An Energy Service Interface for Distributed Energy Resources. *IEEE Conf. on Tech. for Sust.*, 2021.

[15] Carl Shapiro and Srikanth Puttagunta. Field Performance of Heat Pump Water Heaters in the Northeast. 2 2016.

[16] S Bodzin. Air-to-water heat pumps for the home. *Home Energy*, 14(4), 7 1997.

[17] M. Obi, C. Metzger, E. Mayhorn, T. Ashley, and W. Hunt. Nontargeted vs. Targeted vs. Smart Load Shifting Using Heat Pump Water Heaters. *Energies*, 14(22), 2021.

[18] Alexander Belov, Nirvana Meratnia, B Jan van der Zwaag, and Paul Havinga. An Efficient Water Flow Control Approach for Water Heaters in Direct Load Control. *Journal of Engineering & Applied Sciences*, 9(11):2106–2120, 2014.

[19] Kathleen Hudon, Bethany Sparn, Dane Christensen, and Jeff Maguire. Heat Pump Water Heater Technology Assessment Based on Laboratory Research and Energy Simulation Models: Preprint. 01 2012.

[20] Daniel E. Fisher, Simon J. Rees, S. K. Padhmanabhan, and A. Murugappan. Implementation and Validation of Ground-Source Heat Pump System Models in an Integrated Building and System Simulation Environment. *HVAC&R Research*, 12(sup1):693–710, 2006.

[21] Jianhua Fan and Simon Furbo. Buoyancy driven flow in a hot water tank due to standby heat loss. *Solar Energy*, 86(11):3438–3449, 2012.

[22] Sang Hun Lee, Yongseok Jeon, Hyun Joon Chung, Wonhee Cho, and Yongchan Kim. Simulation-based optimization of heating and cooling seasonal performances of an air-to-air heat pump considering operating and design parameters using genetic algorithm. *Applied Thermal Engineering*, 144:362–370, November 2018.

[23] S. Alomani. Power Distribution System Tools for Analyzing Impacts of Projected Electric Vehicle Load Growth Using GridLab-D. Master's thesis, Portland State University, Febraury 2021.

[24] David Wenzhong Gao, Eduard Muljadi, Tian Tian, and Mackay Miller. Software comparison for renewable energy deployment in a distribution network. 2 2017.

[25] D.P. Chassin, P.R. Armstrong, D.G. Chavarria-Miranda, and R.T. Guttromson. Gauss-Seidel accelerated: implementing flow solvers on field programmable gate arrays. In *2006 IEEE Power Engineering Society General Meeting*, pages 5 pp.–, 2006.

[26] A. Clarke. Electric water heater modeling for distributed energy resource aggregation and control. Master's thesis, Portland State University, June 2018.

[27] D. P. Chassin and S. E. Widergren. Simulating demand participation in market operations. In *2009 IEEE Power Energy Society General Meeting*, pages 1–5, 2009.

[28] C. Macal, Prakash Thimmapuraam, Vladimir Koritarov, Guenter Conzelmann, Thomas Veselka, Michael North, Matthew Mahalik, Audun Botterud, and Richard Cirillo. Agent-based modeling of electric power markets. *Proceedings - Winter Simulation Conference*, 2015:276–287, 01 2015.

[29] Donald J Hammerstrom, Ron Ambrosio, Teresa A Carlon, John G DeSteese, Gale R Horst, Robert Kajfasz, Laura L Kiesling, Preston Michie, Robert G Pratt, Mark Yao, Jerry Brous, David P Chassin, Ross T Guttromson, Olof M Jarvegren, Srinivas Katipamula, N T Le, Terry V Oliver, and Sandra E Thompson. Pacific Northwest

Gridwise™ Testbed Demonstration Projects; Part I. Olympic Peninsula Project. 1 2008.

[30] Zachary T Taylor, Krishnan Gowri, and Srinivas Katipamula. GridLAB-D technical support document: Residential end-use module version 1.0. 7 2008.

[31] S Wilcox and W Marion. Users manual for TMY3 data sets (revised). 5 2008.

[32] Nathan D Tenney. Gridlab-d technical support document: Climate module version 1.0. Technical report, Pacific Northwest National Lab.(PNNL), Richland, WA (United States), 2008.

[33] *CTA-2045-B: Modular Communications Interface for Energy Management*. Consumer Technology Association, November 2020.

[34] William Kersting. Radial Distribution Test Feeders. volume 6, pages 908 – 912 vol.2, 02 2001.

[35] Ben Larson, Lucinda Gilman, Robert Davis, Michael Logsdon, Jeffrey Uslan, Ben Hannas, David Baylon, Poppy Storm, Virginia Mugford, and Nick Kvaltine. Residential Building Stock Assessment: Metering Study. Technical report, Northwest Energy Efficiency Alliance, April 2014.

[36] M. C. D. US Census Bureau. Characteristics of New Housing, 2021.

[37] Widder S.H. and M.C Baechler. Impacts of Water Quality on Residential Water Heating Equipment. 2013.

Appendix A: Base Case

The Base case study shows the behavior of the distribution system with a population of EWHs attached to each transformer. The IEEE 13 node feeder comprises 13 nodes distributed in the model. In Section 4.1, only node 633 was discussed. In this Section, two nodes are discussed. These nodes are node 652 and node 684. The delivered apparent power by the transformers associated with these two nodes is shown in this Section for reference.

Node 652 is configured as shown in Figure A.1. Node 652 is a single-phase node that constitutes 40 EWHs attached to five distribution transformers, each rated for 100 kVA. Figure A.3 shows the transformers apparent power of node 652 Phase C. The peak demand of node 652 is 203.7 kVA for the Base case. Further, the energy consumption by the 40 end-use loads associated with node 652, which all constitute EWHs, is 123 kWh.

The feeder model also incorporates a two-phase node, that is node 684. Node 684 is structured as shown in Figure A.2. However, node 684 is configured to include 80 end-use loads and ten transformers, each rated for 100 kVA. Node 684 delivered apparent power for each phase is shown in Figure A.4. Phase A data reveals a peak load of 167 kVA and 162.4 kVA for phase C. The energy consumed by the 80 end-use loads associated with node 684 is 89.3 kWh and 82.2 kWh for phase A and phase C, respectively.

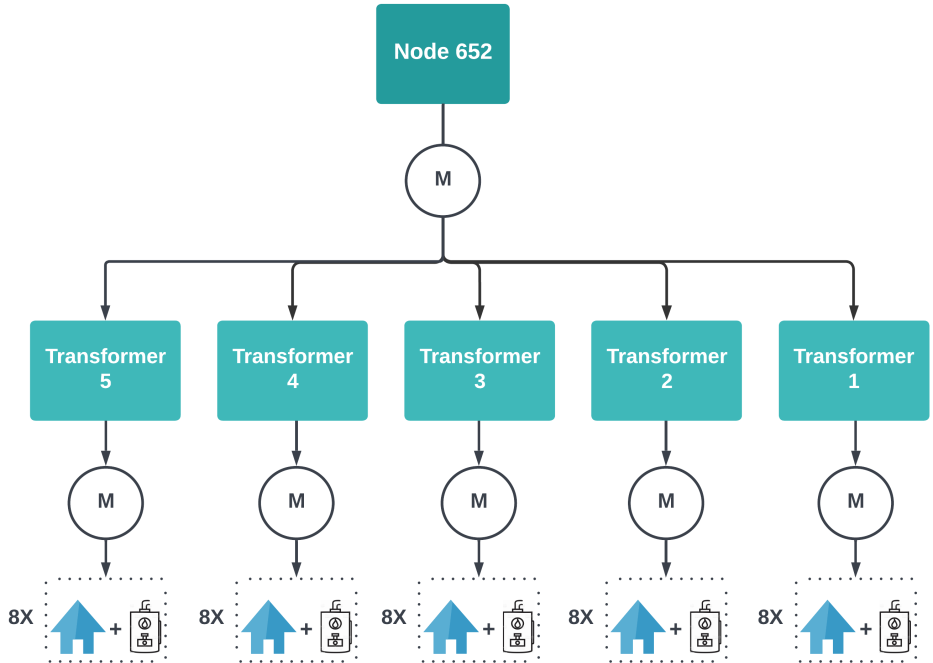

Figure A.1: Node 652 in IEEE 13 Node Test Feeder

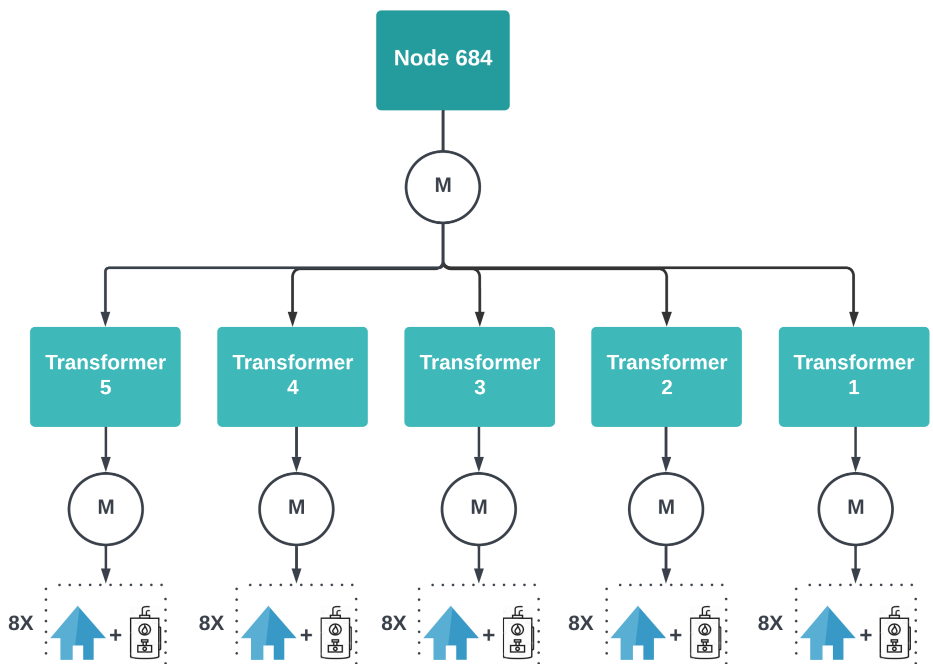

Figure A.2: Node 684 in IEEE 13 Node Test Feeder

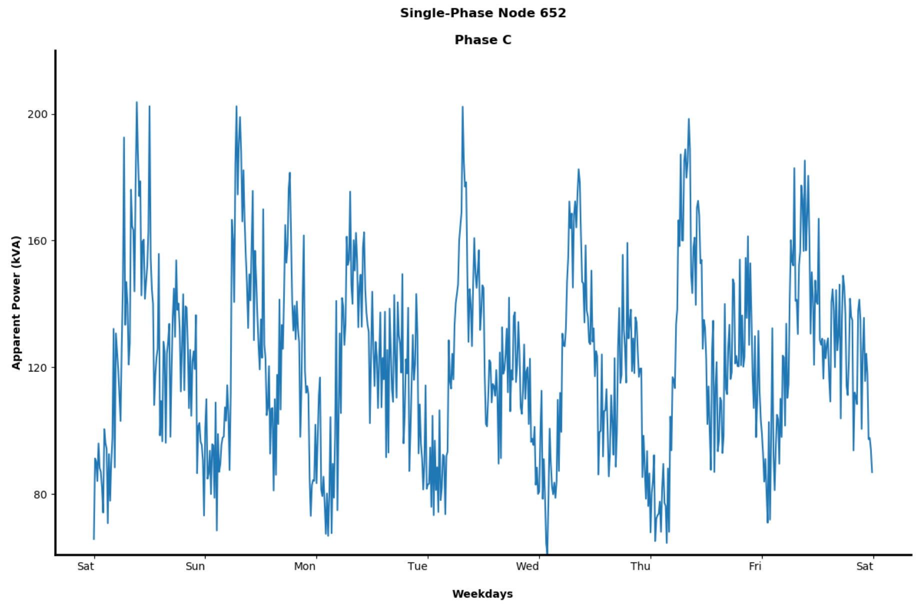

Figure A.3: Base Case: The Distribution Transformers Apparent Power Data in kVA for Node 652

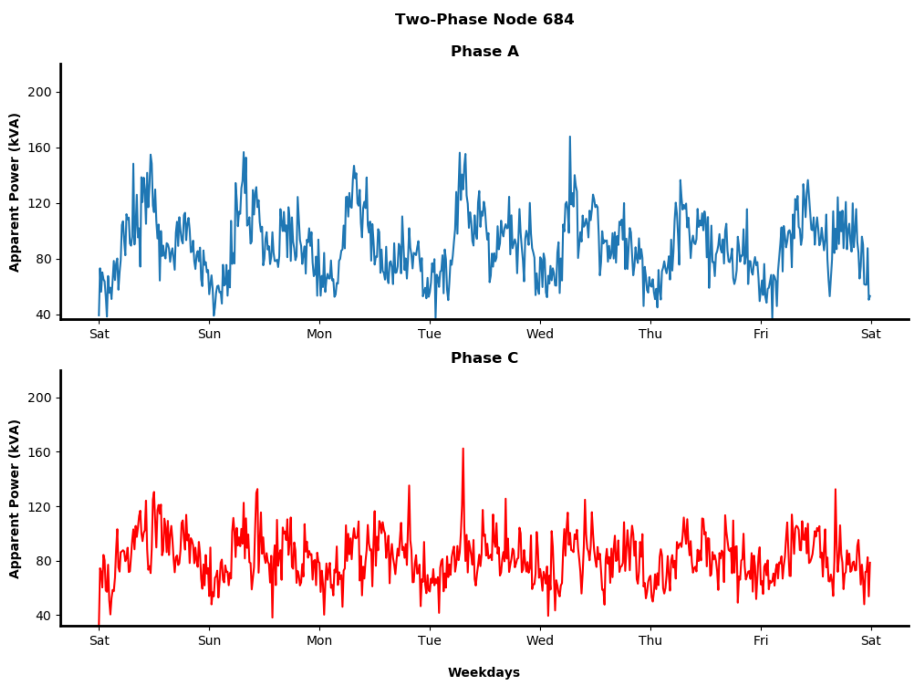

Figure A.4: Base Case: The Distribution Transformers Delivered Apparent Power Data in kVA for Node 684

Appendix B: Heat Pump Water Heater Case Studies

In this Section, all the HPWH penetration cases of nodes 652 and 684 are illustrated. The penetration of HPWHs was implemented in 20% increments. The Base case shows that node 652 is a single-phase node that constitutes 40 end-use loads attached to five transformers. Node 684, on the other hand, includes 80 end-use loads attached to ten distribution transformers. In the following Sections, different levels of HPWHs penetrations are implemented. Starting with 20% of HPWHs in each node, the energy consumption and the peak demand are monitored and compared with the Base case.

B.1 20% Heat Pump Water Heater Case Study

In this case, 20% of HPWHs were distributed in node 652 in the IEEE 13 Node Feeder. Node 652 incorporates eight HPWHs and 32 EWHs. Figure B.1 depicts the energy consumption at the five transformers associated with node 652. The peak demand reported at node 652 with 20% of EWHs replaced by HPWHs was decreased to 199 kVA. The energy consumption by the end-use loads is dropped by only 3% for the 20% HPWH penetration case.

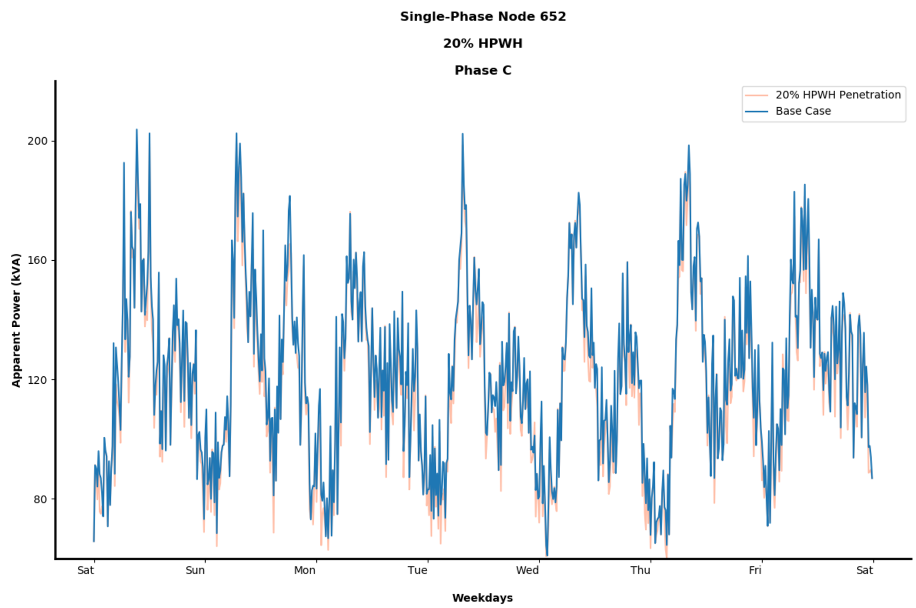

Figure B.1: 20 % HPWHs Penetration: The Distribution Transformers Delivered Apparent Power Data in kVA for Node 652

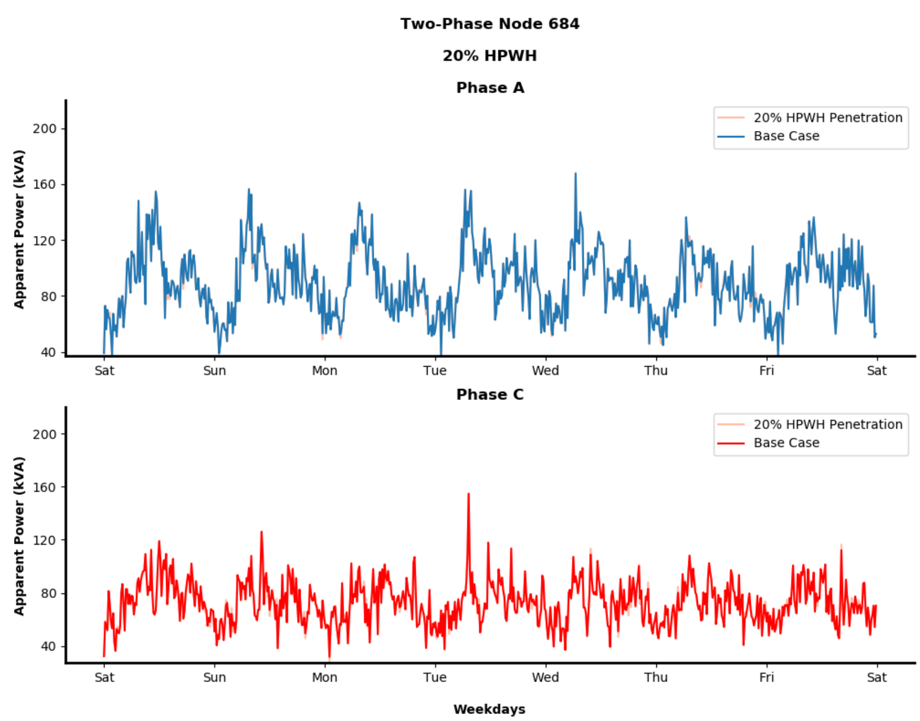

Figure B.2: 20 % HPWHs Penetration: The Distribution Transformers Delivered Apparent Power Data in kVA for Node 684

Similarly, node 684, which incorporates 16 HPWHs and 64 EWHs in phases A and C, shows an insignificant reduction in the peak demand compared to the Base case. The recorded kVA for phase A is 167 and 155 in phase C. Moreover, the energy consumption dropped by 3% and 12% in phases A and C, respectively, as shown in Figure B.2.

B.2 40% Heat Pump Water Heater Case Study

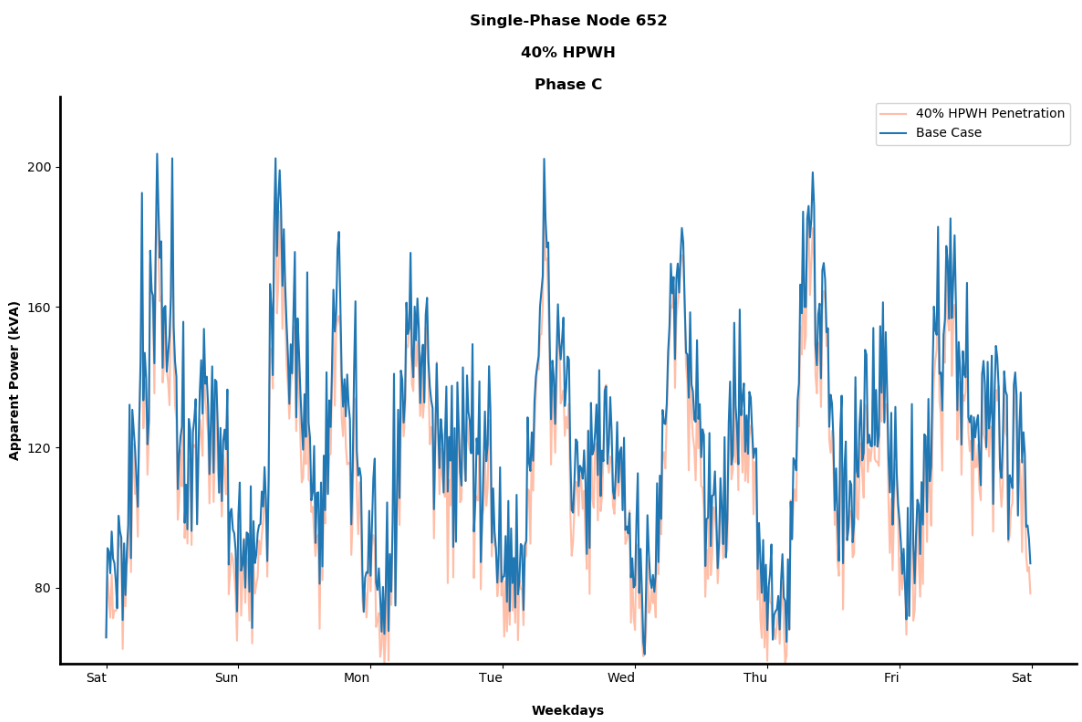

Figure B.3: 40 % HPWHs Penetration: The Distribution Transformers Delivered Apparent Power Data in kVA for Node 652

In this case, 40% of EWHs were replaced by HPWHs in node 652, resulting in 16 HPWHs and 24 EWHs units. Compared to the Base case, Figure B.3 shows that the peak demand was mitigated by 4%. Also, the energy consumption when 40% of HPWHs are deployed in node 652 is reduced by 7%.

As expected, the peak demand in node 684 phase A was reduced due to the 40% HPWH penetration. As illustrated in Figure B.4, phase A shows that the peak demand reached 154 kVA, which results in an 8% reduction. The energy consumption of the end-use loads deployed within node 684 phase A is 85 kWh, which constitutes to 5% decrease from the Base case. Phase C in node 684, however, behaved differently in the 40% HPWH penetration case. The energy consumption of the end-use loads was reduced by 20%. The peak demand of phase C in node 684 is reported as 130 kVA.

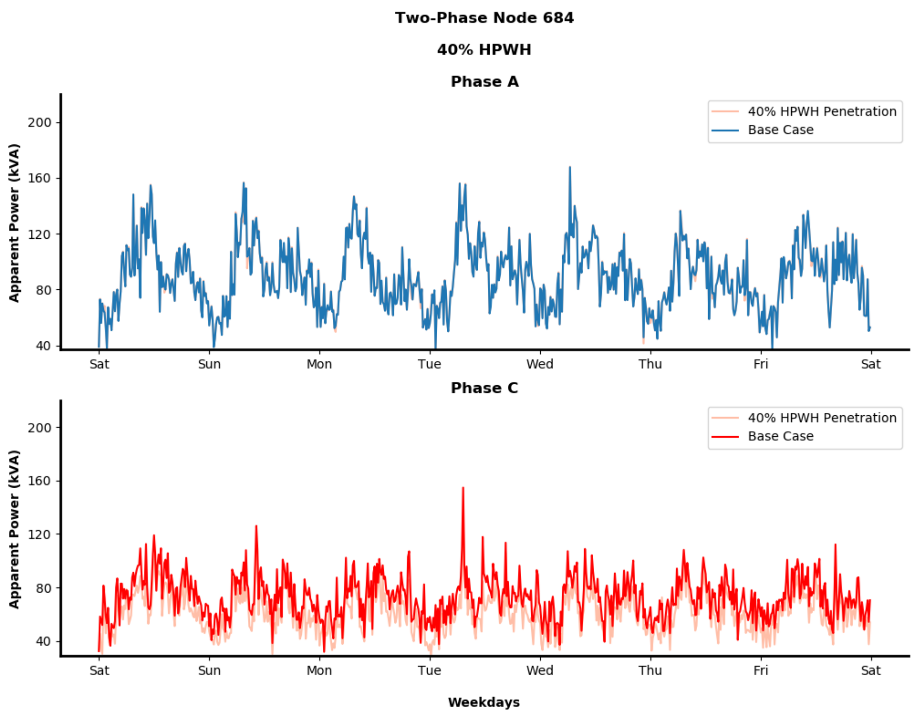

Figure B.4: 40 % HPWHs Penetration: The Distribution Transformers Delivered Apparent Power Data in kVA for Node 684

B.3 60% Heat Pump Water Heater Case Study

Figure B.5 depicts the delivered apparent power in kVA due to 60% of HPWHs penetration. As the HPWH penetration level increases, the peak demand and the energy consumption are expected to decline. The deployment of water heaters in each house is in favor of the HPWH for the 60% penetration case.

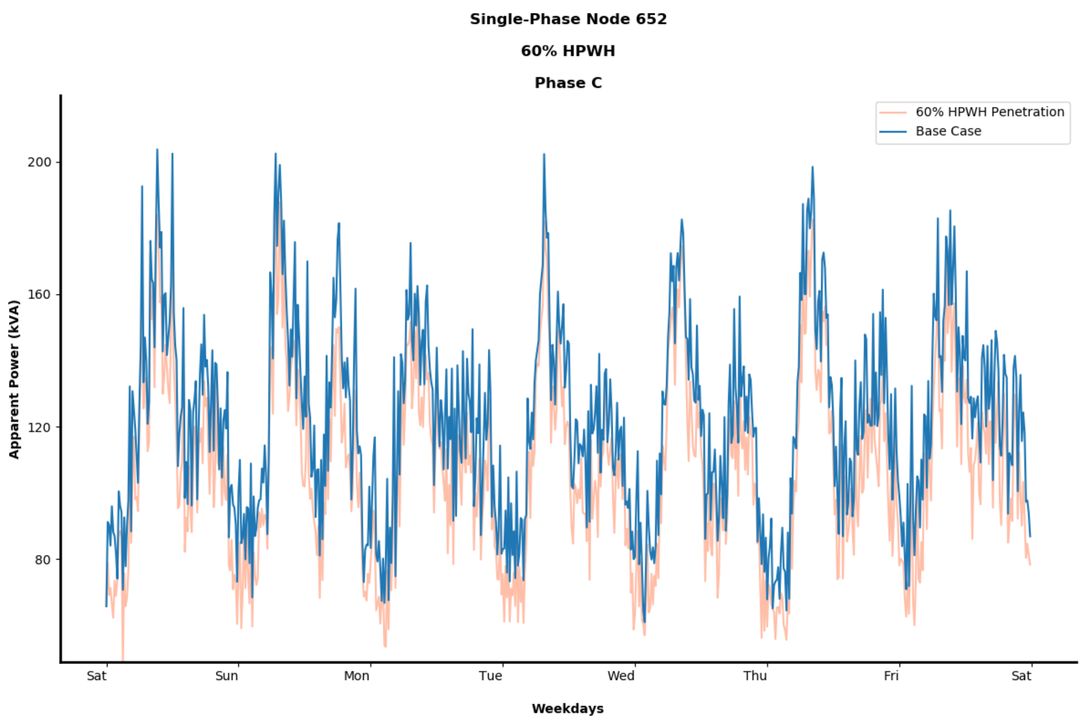

Figure B.5: 60 % HPWHs Penetration: The Distribution Transformers Delivered Apparent Power Data in kVA for Node 652

Therefore, the peak demand measured at node 652 for phase C is dropped by 6.1%. Further, the energy consumption for the mix of water heaters populated in node 652 phase C is decreased by 12.2%. On the other hand, node 684 in this case incorporates 48 HPWHs and 32 EWHs. The peak demand measured at phase A is 150 kVA and 125 kVA for phase C, shown in Figure B.6. These values constitute a 10% and 23% reduction compared to phase

A and phase C in the Base case. The energy consumption by the end-use loads was further decreased by 7% for phase A and 23% for phase C.

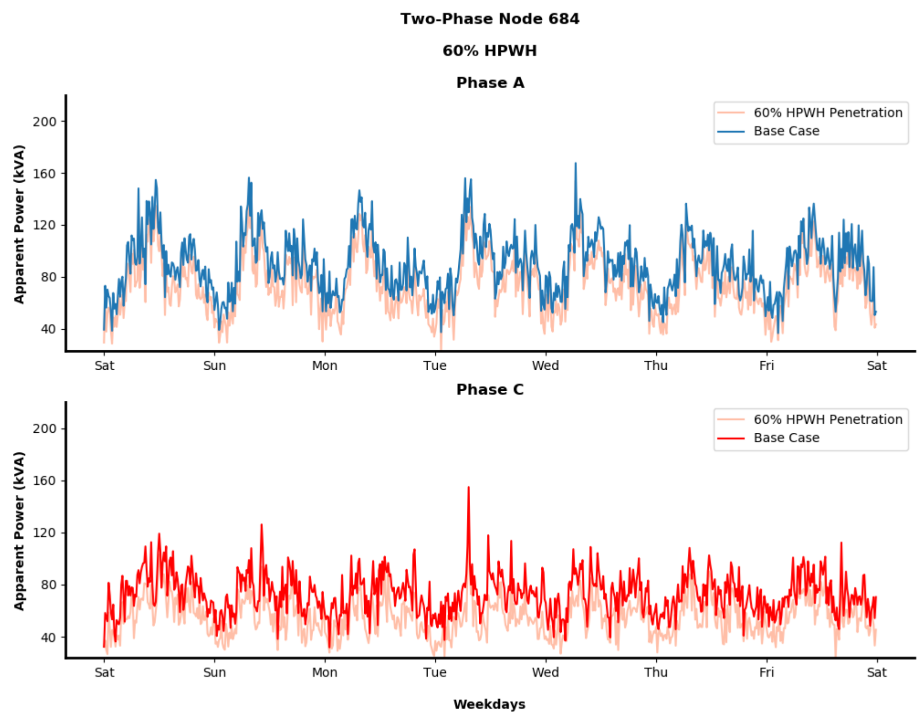

Figure B.6: 60 % HPWHs Penetration: The Distribution Transformers Delivered Apparent Power Data in kVA for Node 684

B.4 80% Heat Pump Water Heater Case Study

Figure B.7 illustrates the delivered apparent power by the transformers associated with node 652. Since the majority of water heaters have been in favor of the HPWH from the 60% penetration case, the peak demand and the energy consumption reduction are noticeable. The reduction in peak demand, in this case, reached 184 kVA, which is a 10% reduction compared to the Base case. Similarly, the energy consumption by the end-use loads was reduced by 17%.

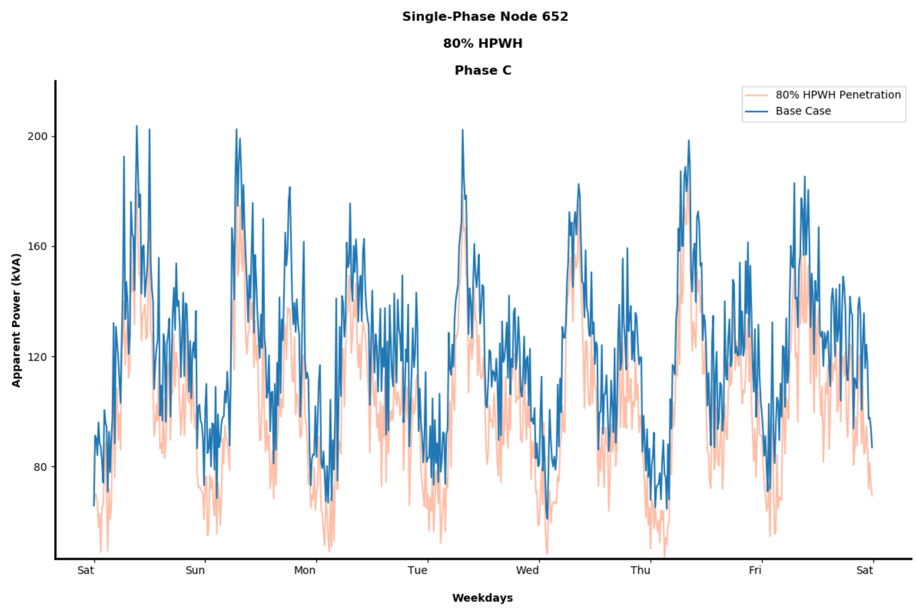

Figure B.7: 80 % HPWHs Penetration: The Distribution Transformers Delivered Apparent Power Data in kVA for Node 652

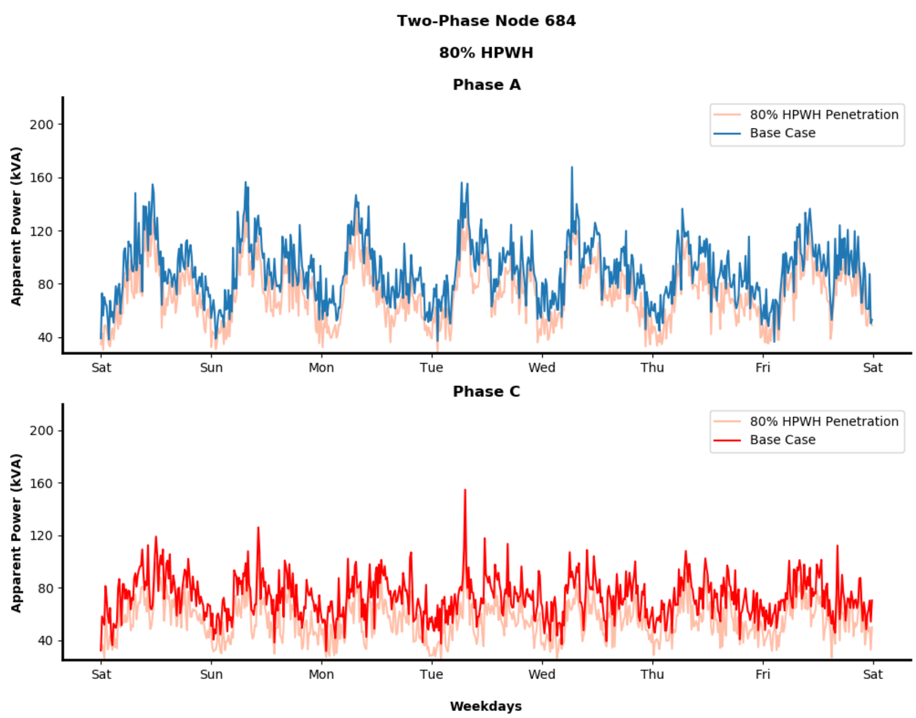

Figure B.8: 80 % HPWHs Penetration: The Distribution Transformers Delivered Apparent Power Data in kVA for Node 684

In a similar manner, node 684 shows an energy reduction in Phases A and C. In Phase A, the energy consumption is reduced by 18%. Similarly, the energy consumption is reduced by 34% in Phase C. The peak demand in phases A and C was reported as 147 kVA and 122 kVA, shown in Figure B.8.

B.5 100% Heat Pump Water Heater Case Study

All the EWHs deployed in each house within nodes 652 and 684 are of type HPWH for the 100% penetration case. Node 652 includes 40 HPWHs, one in each house object. Further, node 684 includes 80 HPWHs. The peak demand in node 652 was reported as 176 kVA, shown in Figure B.9. The energy consumption by the end-use loads was reduced to 96 kWh. Note that, compared to the Base case, these values constitute a 13% and 22% reduction in peak demand and the energy consumption. Node 684 shows a significant reduction. Figure B.10 shows that the peak demand in Phases A and C were reported as 131 kVA and 116 kVA, which constitute 22% and 29% less peak demand than the Base case. Similarly, the energy consumption by the end-use loads was reduced by 28% and 38% in phases A and C.

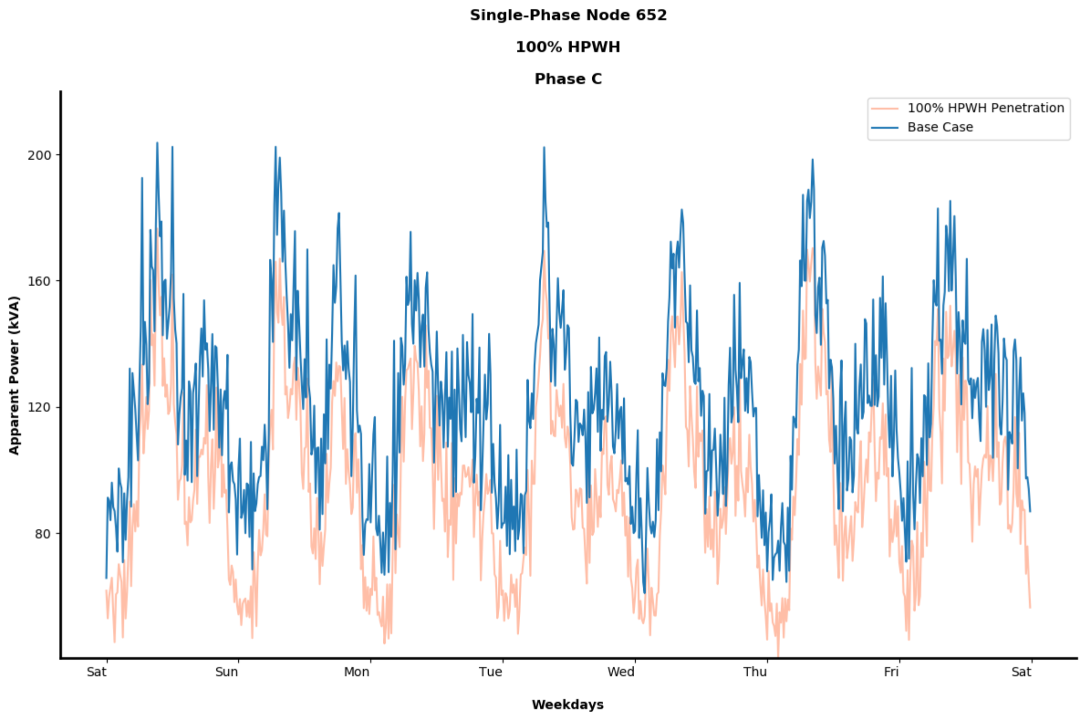

Figure B.9: 100% HPWHs Penetration: The Distribution Transformers Delivered Apparent Power Data in kVA for Node 652

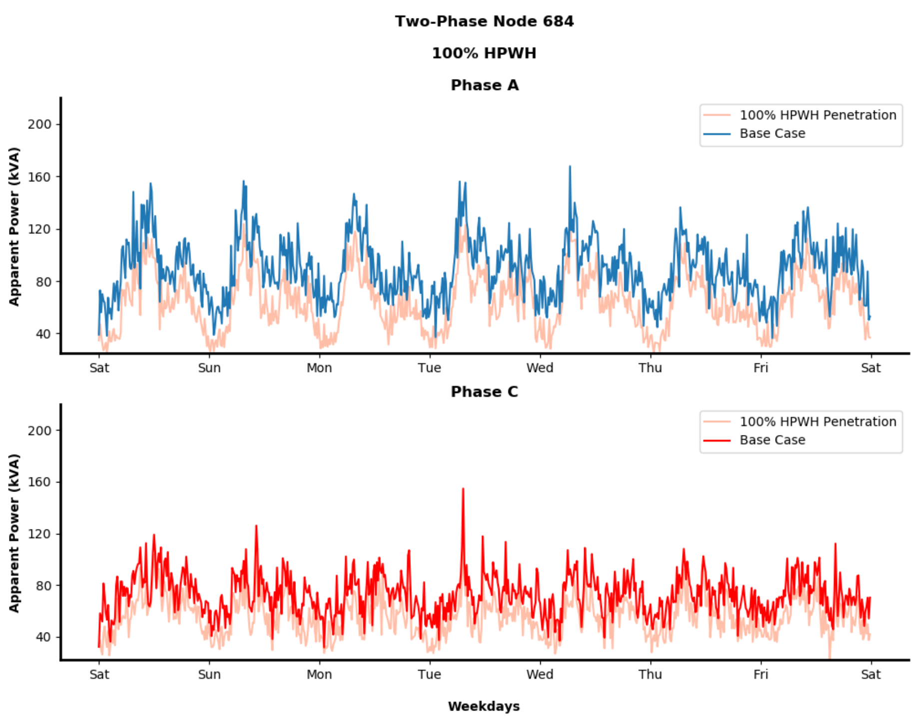

Figure B.10: 100% HPWHs Penetration: The Distribution Transformers Delivered Apparent Power Data in kVA for Node 684

B.6 Results Summary

B.6.1 Node 652

Table B.1: Summary of Peak Load Mitigation in Node 652

Case Study	Peak Load in kVA in Each Phase	Percentage of Peak Load Reduction
	C	C
Base Case	203.7	
20%	199.1	2.3%
40%	195.4	4.1%
60%	191.3	6.1%
80%	184.9	9.3%
100%	176.5	13.1%

Table B.2: Summary of Energy Consumption by End-Use Loads in Node 652

Case Study	Energy Consumption by End-Use Loads (kWh)	Percentage of Energy Consumption by End-Use Loads
	C	C
Base Case	122.2	
20%	118.1	3.4%
40%	113.4	7.2%
60%	107.3	12.2%
80%	101.8	16.7%
100%	95.9	22.1%

B.6.2 Node 684

Table B.3: Summary of Peak Load Mitigation in Node 684

Case Study	Peak Load in kVA in Each Phase		Percentage of Peak Load Reduction in Each Phase	
	A	C	A	C
Base Case	167.6	162.5		
20%	166.9	154.7	0.4%	4.8%
40%	153.6	130.3	8.4%	19.4%
60%	150.2	125.3	10.4%	22.9%
80%	147.2	121.8	12.2%	25.1%
100%	130.9	115.6	21.9%	28.9%

Table B.4: Summary of Energy Consumption by End-Use Loads in Node 684

Case Study	Energy Consumption by End-Use Loads (kWh)		Percentage of Energy Consumption by End-Use Loads	
	A	C	A	C
Base Case	89.3	82.2		
20%	87.1	72.7	2.5%	11.6%
40%	84.5	68.3	5.4%	16.9%
60%	83.2	63.1	6.8%	23.2%
80%	73.02	54.4	18.1%	33.8%
100%	64.1	50.8	28.2%	38.2%